AUS DEM LEHRSTUHL
FÜR DERMATOLOGIE
PROF. DR. MED. MARK BERNEBURG
DER FAKULTÄT FÜR MEDIZIN
DER UNIVERSITÄT REGENSBURG

THE ROLE OF THE HIPPO SIGNALING PATHWAY IN MERKEL CELL CARCINOMA

Inaugural – Dissertation
zur Erlangung des Doktorgrades
der Zahnmedizin

der
Fakultät für Medizin
der Universität Regensburg

vorgelegt von
Monika Dorothee Hoffmann

2020

AUS DEM LEHRSTUHL
FÜR DERMATOLOGIE
PROF. DR. MED. MARK BERNEBURG
DER FAKULTÄT FÜR MEDIZIN
DER UNIVERSITÄT REGENSBURG

THE ROLE OF THE HIPPO SIGNALING PATHWAY IN MERKEL CELL CARCINOMA

Inaugural – Dissertation
zur Erlangung des Doktorgrades
der Zahnmedizin

der
Fakultät für Medizin
der Universität Regensburg

vorgelegt von
Monika Dorothee Hoffmann

2020

Dekan:	Prof. Dr. Dirk Hellwig
1. Berichterstatter:	PD Dr. Sebastian Haferkamp
2. Berichterstatter:	PD Dr. Jens Werner
Tag der mündlichen Prüfung:	08.12.2020

Für meine Eltern

Zusammenfassung:

Das Merkelzellkarzinom (MCC) ist ein seltener und hochaggressiver neuroendokriner Hautkrebs. Das Verständnis der molekularen Pathogenese des MCC ist zum jetzigen Zeitpunkt noch begrenzt. Um die Relevanz des Hippo-Signalweges im Merkelzellkarzinom zu beurteilen, wurde die Expression des yes-assoziierten Proteins (YAP), dem Haupteffektor des Signalweges, ermittelt.

In der vorliegenden Arbeit wurden immunhistochemische Untersuchungen von 47 Tumorgewebeproben und Western Blot-Analysen von 5 MCC-Zelllinien durchgeführt. In allen getesteten Gewebeproben und Zelllinien war keine YAP-Expression nachweisbar. Für Immunfluoreszenzexperimente wurden zwei MCC-Zelllinien in Suspension mit Hilfe von Poly-L-Ornithin (PLO) auf Objektträger aufgebracht. Die Zellen wurden anschließend mit einer Plasmid-DNA, die YAP enthielt, und dem entsprechenden Leervektor als Negativkontrolle transfiziert. Die Transfektion wurde durchgeführt, um den Einfluss von YAP auf die Proliferation von MCC-Zellen zu untersuchen. Ki-67 diente hierbei als Proliferationsmarker und wurde in einem Immunfluoreszenz-Experiment analysiert. Die Untersuchungen ergaben, dass die mit dem YAP-Plasmid und seinem leeren Vektor transfizierten Zelllinien keine signifikanten Unterschiede in der Expression von Ki-67 aufwiesen.

Zusammenfassend zeigen die erhobenen Daten, dass der Hippo-Signalweg an der Entstehung des MCC nicht beteiligt ist. Weitere immunologische und molekulare Studien sind notwendig, um ein umfangreicheres Verständnis der Tumorentstehung des Merkelzellkarzinoms zu gewinnen.

Table of contents

1 Introduction

1.1 Merkel cell carcinoma

Merkel cell carcinoma (MCC) is a rare and aggressive tumor of the skin that occurs mostly in elderly patients (1). MCC metastasizes early and there are no curative therapies for patients with distant metastases. Therefore, it is crucial to identify the molecular mechanisms that drive transformation and invasion of the MCC (2). The incidence of MCC in Europe is 0.13/100 000 per year and up to 1.6/100 000 per year in Australia. There are slightly more men affected than women (3). The tumor occurs mainly on the head and neck (about 50% of cases) or the extremities (30%) since UV light is an important risk factor (4,5). Another factor increasing the risk for developing MCC is disease-related or iatrogenic immunosuppression (6).

Primary MCCs present as a rapidly growing, purple/red/blue dome-shaped or plaque-like lesion with firm consistency and a shiny surface. The name MCC stems from its histological and immunohistochemical similarity to the Merkel cells of the skin (7). The acronym “AEIOU” (asymptomatic; rapid expansion; immunosuppressed, older patient; UV-light exposure) summarizes the typical clinical characteristics of MCC (8).

In 2008, the discovery of the Merkel cell polyomavirus (MCPyV), that is clonally integrated into the genome of the cancer cells in a majority of MCC (80%), was a milestone in understanding the etiology of the tumor (9). MCPyV is encoding T antigens, that can induce carcinogenesis by acting on cellular tumor-suppressor proteins (10).

The typical histology of the MCC shows small, round to oval cells with a vesicular nucleus and hardly any cytoplasm. The cancer appears in a wide variety of histopathological patterns; therefore, a definitive diagnosis usually requires immunohistochemical staining. Cytokeratin 20 (CK20) is the most used marker in routine diagnostics (11).

1.2 Role of YAP in the Hippo signaling pathway

The Hippo signaling pathway was initially identified through the examination of mutant tumor suppressors in drosophila flies. A strong tissue growth was found as a result of diminished cell death and increased cell proliferation, due to loss-of-function mutations of parts of the Hippo pathway (12). The discovery that this pathway and its effect on cell proliferation is active in mammals provoked great interest, as experiments have shown that the Hippo pathway is strongly involved in a wide variety of cancer processes and has an immense influence on regulatory functions in the development of organs, stem cell biology and regeneration (13–16).

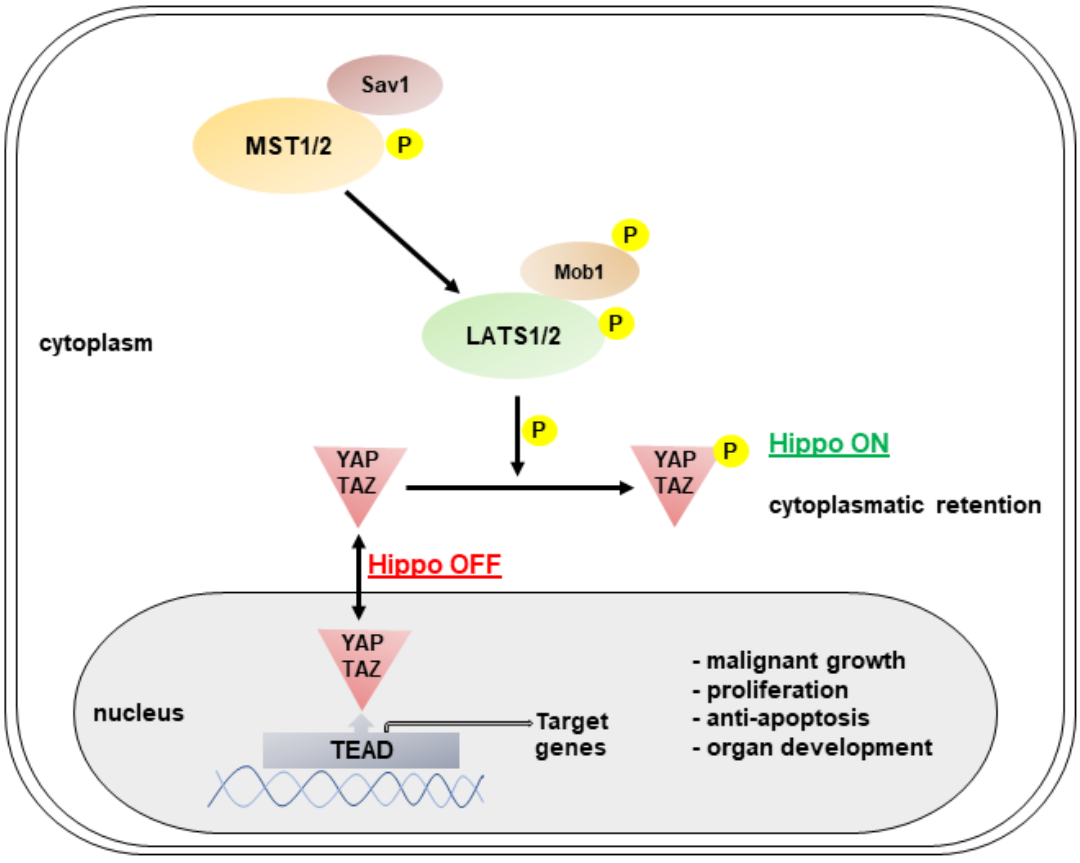

Figure 1 Hippo signaling pathway

Core components of the Hippo signaling pathway in mammals are illustrated. When Hippo signaling is activated, LATS1/2 phosphorylate YAP/TAZ, which results in the retention of YAP/TAZ in the cytoplasm. On the contrary the Hippo signaling pathway is inactive when YAP is hypophosphorylated, YAP/TAZ translocates to the nucleus and interacts with TEAD resulting in the expression of YAP/TAZ target genes. Adapted from Gumbiner et al. (13)

Table 1 Components of Hippo signaling pathway in mammals and drosophila

Adapted from Pan et al. (12)

Mammals	Drosophila	Conserved Domains of mammal components
MST1, MST2 (STK4, STK3)	Hippo	Ste20 Ser/Thr kinase domain
LATS1, LATS2	Warts	NDR Ser/Thr kinase domain
YAP, TAZ (WWTR1)	Yorkie	WW and TEAD-binding domain
Sav1 (WW45)	Salvador	WW domain
Mob1	Mats	Mob1 domain
TEAD	Scalloped	TEA and YAP binding domain

The core of the Hippo signaling pathway consists of a serine-threonine (Ser/Thr) kinase cascade with linked scaffolding and/or regulatory proteins that affect a transcriptional module that regulates the expression of genes controlling growth (17). The kinase module includes the mammalian orthologues of Drosophila melanogaster Hippo, mammalian STE20-like protein kinase 1 and 2 (MST1 and MST2, also known as STK4 and STK3). Additionally, it activates another kinase, the large tumor suppressor 1 (LATS1) and LATS2 (Warts in flies). The latter phosphorylates the transcriptional module, including yes-associated protein (YAP) and transcriptional co-activator with PDZ-binding motif (TAZ; also known as WW domain-containing transcription regulator protein 1: WWTR1) which is the orthologue to Yorkie in Drosophila. YAP and TAZ are two closely related paralogues that mostly mediate the downstream effects of the pathway. Therefore, they are often taken as a measure of the activity of the Hippo signaling pathway (12). The scaffolding proteins that are needed for the activity of the Hippo pathway consist of the WW domain-containing protein Sav1 (also called WW45) and the adaptor protein Mob1 (18,19).

The two co-activators YAP and TAZ are the major effectors of the pathway, that shuttle between the nucleus and the cytoplasm (20). In the nucleus, YAP interacts with transcription factors of the TEA domain family (TEAD), which is the orthologue to Scalloped in flies. The TEA domain family members induce the expression of anti-apoptotic and growth promoting genes. Its phosphorylation state determines the translocation of YAP. LATS1 and LATS2 inactivate YAP by phosphorylation. The Hippo kinase module is ‘on’, and the output gene production is deactivated. On the contrary, the Hippo signaling pathway is ‘off’ when YAP is hypophosphorylated. In this case, YAP translocates to the nucleus and induces target gene expression (16).

YAP, as a key component of the Hippo signaling pathway, affects the regulation of organ size, regeneration, tissue homeostasis and tumorigenesis (21–23). In recent years, studies have shown that the Hippo signaling pathway should not be seen as a simple linear pathway (22). If anything the pathway is a complex construct wherein YAP functions as a central component, that integrates signals from various upstream signaling pathways, other cancer-relevant pathways, cell-cell interactions and mechanical forces. By binding and activating to different downstream transcriptional factors, YAP controls cell social behaviour and cell-cell interactions (12,22,24).

1.3 Aim of the study

The Hippo signaling pathway is an important tumor-suppressor pathway, and its failure has been associated with a variety of different cancers, in which YAP conditions cancerous cells to overcome contact inhibition and to enable uncontrollable growth (24). Studies have shown, that the dysregulation of the Hippo signaling pathway is playing an important role in a wide range of skin cancers, such as basal and squamous cell carcinoma and cutaneous melanoma (25,26). This study aims to investigate the role of the Hippo signaling pathway in the pathogenesis of Merkel cell carcinoma.

2 Material and methods

2.1 Material

2.1.1 Tissue samples

For immunohistopathological analyses, forty-seven formalin-fixed and paraffin-embedded primary and metastatic MCC patient samples were used. Human testis tissue served as a positive control. All tissue samples were kindly provided by the Biobank of the Department of Dermatology, University Medical Center Regensburg.

2.1.2 Solutions and reagents

Table 3 Solutions and reagents

label	**manufacturer & headquarter**	**materialno.**
Acridine Orange (AO)/ Propidium Iodide (PI) Stain	Logos Biosystems, Anyang (South Korea)	F23001
AEC plus high sensitivity substrate chromogen ready to use	Dako REAL™, Santa Clara CA (USA)	K3469
Albumin Fraktion V (BSA)	Carl Roth GmbH &Co KG, Karlsruhe	8076.3
Antibody Dilution Buffer Immunofluorescence (IF): 1x Phospate Buffered Saline (PBS) 1% BSA 0,3% Triton X-100		
Antibody Diluent	Zytomed System GmbH, Berlin	ZUCO 25-100
Aquatex mounting media	Merck KGaA, Darmstadt	1.085.620.050
Blocking Buffer (IF): 1x PBS 5% BSA 0.3% Triton X-100		

1x Blocking Buffer (Western Blot): 1x Tris buffered Saline (TBS) 1%Tween 20 5 % BSA Adjust pH to 7.5		
1x Blotting Buffer: 100 ml 10x Tris/Glycine Buffer (25 mM Tris, 192 mM Glycine, pH 8.3)	BIO-RAD Laboratories Inc., Hercules, CA (USA)	161-0771
200 ml Methanol 700 ml distilled water (ddH_20)	Fisher Scientific International Inc., Pittsburgh PA (USA)	M\4000\17
Bromophenol blue	Sigma-Aldrich, St. Louis, MO (USA)	B0126
Complet 25x One tablet was dissolved in 2 ml ddH_20	F.Hoffmann - La Roche AG, Switzerland	4693116001
Dimethylsulfoxide (DMSO)	Sigma-Aldrich, St. Louis, MO (USA)	D4540
distilled water (ddH_20)	University Hospital Regensburg	
Dithiothreitol (DTT)	Sigma-Aldrich, St. Louis, MO (USA)	D0632
Dulbecco Phosphate Buffered Saline, (DPBS) (1x)	Gibco™,Thermo Fisher Scientific Inc., Waltham, MA (USA)	14190-094
Eosin	Sigma-Aldrich, St. Louis, MO (USA)	HT 110116
Ethanol denatured	Chemikalienausgabe University Regensburg	
Ethanol p.a. 99,8%	Sigma-Aldrich, St. Louis, MO (USA)	V001495
Fetal Cow Serum (FCS) FETAL + High Performance	Anprotec, Bruckberg	AC-SM-0161
Formaldehyde 4% buffered	Merck KGaA, Darmstadt	100496
Glycerol	Sigma-Aldrich St. Louis, MO (USA)	G7757
Hydrochloric acid (HCl)	Titripur®, Merck KGaA, Darmstadt	1.090.571.000
HIER Citrat Buffer pH 6	Zytomed Systems GmbH, Berlin	ZUCO28
Hydrogen peroxide (H_2O_2) 100 volumes >30%	Fisher Scientific International Inc., Pittsburgh PA (USA)	1404697

Kanamycin-Sulfat	Sigma-Aldrich St. Louis, MO (USA)	60615
L-Glutamine solution	Sigma-Aldrich St. Louis, MO (USA)	G7513
5x SDS-PAGE Protein Loading Buffer (Reducing): 250 mM Tris-HCl pH 6.8 50% Glycerol 10% Sodium dodecyl sulfate (SDS) 0.5% Bromophenol blue 200 mM DTT (add freshly)		
Mayer´s hemalum solution	Carl Roth GmbH & Co. KG, Karlsruhe	T865.3
Mounting Media Roti-Mount-FluorCore Dapi	Carl Roth GmbH & Co. KG, Karlsruhe	HP20.1
PageRuler Prestained Protein Ladder	Thermo Fisher Scientific Inc., Waltham, MA (USA)	26616
Paraformaldehyde	Sigma-Aldrich St. Louis, MO (USA)	158127
Penicillin-Streptomycin (PS)	Sigma-Aldrich St. Louis, MO (USA)	P0781
Potassium chloride (KCl)	Merck KGaA, Darmstadt	104936
p-Xylol	Merck KGaA, Darmstadt	808691
Phosphate Buffered Saline (PBS) Dulbecco	Merck KGaA, Darmstadt	L182-05
PhosSTOP 10x One tablet was dissolved in 1 ml ddH_20	F.Hoffmann - La Roche AG, Basel (Switzerland)	4906845001
Poly-L-Ornithine solution (PLO)	Sigma-Aldrich St. Louis, MO (USA)	P4957
Ponceau S Solution	Sigma-Aldrich St. Louis, MO (USA)	P7170
2x Radioimmunoprecipitation assay (RIPA) Stock solution: 100 mM Tris-HCl pH 7.5 300 mM NaCl 2% Triton X-100 0,2% SDS 1% Sodium Deoxycholate		

1xRIPA: 1000 µl 2x RIPA 80 µl Complet 25x 200 µl PhosSTOP 10x 100 µl 10% Sodium deoxycholate 620 µl ddH_20		
Roti-Liquid Barrier Marker	Carl Roth GmbH & Co. KG, Karlsruhe	AN92.1
RPMI-1640 Media	Sigma-Aldrich St. Louis, MO (USA)	R8758
1x Running Buffer: 100 ml 10x TGS Buffer 900 ml ddH_20	BIO-RAD Laboratories Inc., Hercules CA (USA)	161-0732
Sodium dodecyl sulfate (SDS) pellets	Carl Roth GmbH & Co. KG, Karlsruhe	CN30.3
Sodium Deoxycholat	Sigma-Aldrich St. Louis, MO (USA)	D6750
Sodium chloride (NaCl)	Carl Roth GmbH & Co. KG, Karlsruhe	3957.1
20x Tris buffered saline (TBS): 2.74 M NaCl 53.66 mM KCl 380.71 mM Tris Base Adjust pH to 7.5		
Tris hydrochloride	Sigma-Aldrich St. Louis, MO (USA)	10812846001
Triton 2%	Sigma-Aldrich St. Louis, MO (USA)	T9284
Triton X-100	Sigma-Aldrich St. Louis, MO (USA)	T8787
Trypsin-EDTA Solution	Sigma-Aldrich St. Louis, MO (USA)	T4174
Tween 20	Carl Roth GmbH & Co. KG, Karlsruhe	9127.1
Washing Buffer (TBS-T): 10 ml 10% Tween 20 50 ml 20x TBS 940 ml ddH_20 Adjust pH to 7.5		

2.1.3 Media and agarose plates

Table 4 Media and agarose

label	manufacturer and headquarter	materialno.
LB-Media (Lennox) 20 g LB-Media, fill up to 1 liter with ddH_20, autoclave	Carl Roth GmbH & Co. KG, Karlsruhe	X964.3
Ultra Pure Agarose	Invitrogen AG Carlsbad CA (USA)	16500-500

2.1.4 Vectors

Table 5 Vectors

label	source
pEGFP-C3-hYAP1	was a gift from Marius Sudol Addgene plasmid # 17843 http://n2t.net/addgene:17843 RRID:Addgene_17843 (27)
pEGFP-C3	was a gift from working group Witzgall Institute for Molecular and Cellular Anatomy University of Regensburg

2.1.5 Kits

The kits shown in the following table were always performed according to their instructions.

Table 6 Kits

label	**manufacturer and headquarter**	**materialno.**
K2 Transfection System	Biontex Laboratories GmbH, München	T060-1.0
Lipofectamine 3000 Transfection Kit	Invitrogen AG Carlsbad, CA (USA)	L3000-008
Nucleo Bond PC20 Buffer S1: 50 mM Tris HCl pH 8.0 10 mM EDTA 100 µg RNase A stored at 4°C Buffer S2: 200 mM Sodium hydroxide (NaOH) SDS stored at room temperature Buffer S3: 3.0M Potassium acetate pH5.5 stored at 4°C	Marcherey Nagel, Düren	740.571.100
Pierce BCA Protein Assay Kit	Thermo Fisher Scientific, Waltham, MA (USA)	23225
Roti-Histokitt II	Carl Roth GmbH & Co. KG, Karlsruhe	T 160.1
Western Bright ECL	Advansta Inc. San Jose, CA (USA)	160927-51
Zytochem Plus HRP Kit / Rabbit	Zytomed Systems GmbH, Berlin	HRP060-Rb

2.1.6 Antibodies

Table 7 Antibodies

label	manufacturer and headquarter	materialno.
Alexa Flour 594 Goat Anti-Mouse	Thermo Fisher Scientific, Waltham MA (USA)	A-11032
β-Actin (C4)	Santa Cruz Biotechnology Inc., Dallas TX (USA)	sc-47778
Cytokeratin 20 (CK20) (KS20.8) Mouse monoclonal Antibody (mAb)	Leica Biosystems, Wetzlar	PA0022
Ki-67 (8D5) Mouse mAb	Cell Signaling, Danvers MA (USA)	9449
Peroxidase AffiniPure Donkey Anti-Mouse IgG (H+L)	Jackson Immuno Research Laboratories Inc. West Grove PA (USA)	715-035-150
Peroxidase AffiniPure Donkey Anti-Rabbit IgG (H+L)	Jackson Immuno Research Laboratories Inc. West Grove PA (USA)	711-035-152
Phospho-YAP (p-YAP) (Ser127) (D9W2I) Rabbit mAb	Cell Signaling, Danvers, MA (USA)	13008
Yes associated protein (YAP) (D8H1X) XP Rabbit mAb	Cell Signaling, Danvers, MA (USA)	14074

2.1.7 Primers

The freeze-dried primers were resolved in sterile water to a final concentration of 100 pmol/µl. For further use 10 µM solutions were prepared. Following primers were designed to sequence YAP on pEGFP-C3-hYAP1.

Table 8 Primers

YAP Sequencing (Seq.) Primers:

label and sequence	**manufacturer and headquater**	**materialno.**
YAP1 Seq.1 neu 5'-GGAGCTGTACAAGTCCGGAC-3'	Seqlab GmbH a susidiary of Microsynth AG, Balgach (Switzerland)	3591583
YAP1 Seq.2 5'-CAGCTTCTCTGCAGTTGGGA-3'	Seqlab GmbH a susidiary of Microsynth AG, Balgach (Switzerland)	3591580
YAP1 Seq.3 5'-TCATGGGTGGCAGCAACTC-3'	Seqlab GmbH a susidiary of Microsynth AG, Balgach (Switzerland)	3591582

2.1.8 Cell lines

Table 9 Cell lines

type	cell line
Merkel cell carcinoma:	MKL-1
	MKL-2
	MS-1
	PeTa
	WaGa
Malignant melanoma:	A375

2.1.9 Bacteria

Table 10 Bacteria

label	manufacturer and headquarter	materialno.
Escherichia coli (E.coli) DH5α	Thermo Fisher Scientific, Waltham MA (USA)	18258012

2.1.10 Databases and softwares

Table 11 Databases and softwares

label	manufacturer and headquarter
AxioVision SE64 Rel.4.9	Carl Zeiss Microimaging GmbH, Jena
Citavi 6	Citavi, Wändenswil (Switzerland)
DNA Dynamo Sequence Analysis Software	BlueTractor Software Ltd., North Wales (UK)
Excel 2019	Microsoft Corporation, Redmond, WA (USA)
Fiji ImageJ	Fiji, Milwaukee, WI (USA)
GraphPad Prism 6	Graphpad Software Inc., San Diego, CA (USA)
ImageLab	BIO-RAD Laboratories Inc., Hercules, CA (USA)
Luna™ Dual Fluorescence	Logos Biosystems, Anyang (South Korea)
Microsynth Seqlab	Microsynth Seqlab, Göttingen
NanoDrop 2000	Thermo Fisher Scientific, Waltham, MA (USA)
PowerPoint 1909	Microsoft Corporation, Redmond, WA (USA)
VarioSkan Flash	Thermo Fisher Scientific, Waltham, MA (USA)
Viewpoint light	PreciPoint GmbH, Freising
Word 2019	Microsoft Corporation, Redmond, WA (USA)

2.1.11 Equipment

Table 12 Equipment

label and utilization	manufacturer and headquarter	materialno.
Blotting Chamber Mini PROTEAN 3 cell	BIO-RAD Laboratories Inc., Hercules CA (USA)	/
BOND System Immunostainer	Leica Biosystems, Wetzlar	/
Centrifuge 5415R	Eppendorf AG, Hamburg	/
Centrifuge Universal 320R	Andreas Hettich GmbH &Co. KG, Tuttlingen	/
Chemidoc Imaging System	BIO-RAD Laboratories Inc., Hercules CA (USA)	17001401
Cooling Plate	Microm GmbH, Neuss	CP 60
Digital microscope	PreciPoint, Freising	M8
Dual Fluorescence cell counter Luna fl	Logos Biosystems Anyang (South Korea)	/
Elektrophoresis system Mini PROTEAN tetra system	BIO-RAD Laboratories Inc., Hercules CA (USA)	/
Fluorescence microscope Axio Observer.Z1	Carl Zeiss Microimaging GmbH, Jena	Z1
Incubator HERA cell 240	Thermo Scientific, Waltham, MA (USA)	51026420
Laminar airflow cabinet HERASAFE KS	Thermo Scientific Thermo Electron LED GmbH, Waltham MA (USA)	KS9
Magnetic stirrbar	Heidolph Instruments GmbH & Co KG, Schwabach	MR3001K
Microscope Biomed	Wild Leitz GmbH, Heerbrugg	020-507.01
Microscope Labovert FS	Wild Leitz GmbH, Heerbrugg	090-127.017
Microtom	Microm GmbH, Neuss	HM400R
Multifuge	Thermo Fisher Scientific Heraeus, Waltham, MA (USA)	3 S-R
NanoDrop 2000 Spectrophotometer	Thermo Fisher Scientific Waltham, MA (USA)	/

Pipette Pipetman classic	Gilson Inc., Middleton, WI (USA)	p1000(F123602) p200(F123601) p20(F123600) p10(F144802) p2(F144801)
Pipetting aid easypet	Eppendorf AG, Hamburg	4421
PowerPac HC Power Supply	BIO-RAD Laboratories Inc., Hercules CA (USA)	1645052
Shaker IKA-VIBRAX- VXR electronic	Janke und Kunkel, Staufen im Breisgau	VX7
Steamer Multigourmet	BRAUN, Kronberg	FS10
Thermomixer compact	Eppendorf AG, Hamburg	/
Ultrasonic Bath Qualilab	Merck Eurolab GmbH, Darmstadt	USR 30H
VarioSkan Flash spectral scanning reader	Thermo Fisher Scientific Waltham, MA (USA)	5250030
Water bath	Microm GmbH, Neuss	SB 80

2.2 Methods

2.2.1 Hematoxylin and eosin staining

All paraffin-embedded tissue samples were cut in 2 µm thin sections, mounted on histoslides and incubated at 72°C for 20 minutes. Patient samples were stained with hematoxylin and eosin (HE), as well as the specific monoclonal antibodies YAP and CK20. For hematoxylin and eosin staining, tissue samples were first dehydrated through a descending alcohol series: 2x Xylol (5 min), 2x 100% Ethanol (EtOH) (5 min), 2x 96% EtOH (5 min), 2x 70% EtOH (5 min). Subsequently, they were washed in ddH_2O for 5 minutes and stained in hematoxylin for 12 minutes. Blueing was achieved by rinsing the samples in warm running tap water for 10 minutes. Afterwards, the tissue samples were stained in eosin for 20 seconds (sec) and washed in ddH_2O for 5 seconds. Then, the sections were hydrated through an increasing series of alcohol: 2x 70% EtOH (2 sec), 2x 96% EtOH (2 sec), 1x 100% EtOH (5 min), 2x Xylol (5 min). In the end, Roti-Histokitt was applied to each paraffin section and covered with glass cover slip.

2.2.2 Immunohistochemistry

2.2.2.1 YAP

For YAP staining, tissue samples were also dehydrated through a descending alcohol series: 2x Xylol (5 min), 2x 100% Ethanol (EtOH) (5 min), 2x 96% EtOH (5 min) 2x 70% EtOH (5 min). Afterwards, the endogenous peroxidase was blocked by incubating the sections in 3% H_2O_2 for 10 minutes. After another washing in distilled water for 5 minutes, the samples were boiled in precooked acidic citrate buffer pH 6 for 20 minutes and chilled on ice for 20 minutes before transferring them to PBS for 10 minutes. Subsequently, slides were fixed in coverslides and washed with PBS. From that point on all solutions of the Zytochem Plus HRP Kit were used. Afterwards, samples were blocked at room temperature (RT) for 10 minutes to avoid unspecific antibody binding and were washed with PBS for 5 minutes. Then tissue sections were incubated with anti-YAP primary antibody (1:400) at 4°C overnight. The following day, sections were washed three times with PBS and incubated with anti-rabbit secondary biotinylated antibody at RT for 30 minutes. After three washes with PBS for 5 minutes, samples were incubated with streptavidin-HRP-conjugate at RT for 20 minutes and washed another three times with PBS. Finally, specimens were stained with AEC plus, and the reaction was stopped with distilled water as soon as the positive control showed distinct staining. Mayer´s hemalum solution was used for counterstaining. Finally, mounting-media was applied to the paraffin sections, which were then covered with glass cover slips.

2.2.2.2 Cytokeratin-20

The histomorphology of MCC in hematoxylin and eosin staining appears relatively uncharacteristic. Therefore, immunohistochemical staining to verify the diagnosis is vital. CK20 is an established marker to ensure the presence of MCC. The CK20 staining analysed in this study were kindly provided by the dermatopathological routine of the Department of Dermatology (University Medical Center Regensburg). For antibody staining, the automated BOND system was used according to the manufacturer´s instructions. The CK20 antibody was applied with a concentration of 0.09 mg/l. Counterstaining was achieved with Mayer´s hemalum solution.

2.2.3 Streaking bacteria for single colonies on LB agar plate

The pEGFP-C3-hYAP1 plasmid was delivered as bacterial E.coli stab. To get single colonies, the bacteria were streaked with a sterile inoculating loop on a LB agar plate with kanamycin. Agar plates were made by mixing 7.5 g LB agar, 20 g LB media and distilled water was added to 1 liter. After autoclaving, the solution was chilled down to 50°C and kanamycin (1/1000) was added. Subsequently, petri dishes were filled with liquid agar and as soon as the agar plates were set, they were stored a 4°C. The next day the bacteria were streaked on the LB agar plates.

2.2.4 Preparation of plasmid DNA via Midi Preparation

Plasmids were isolated by using the NucleoBond PC 20-Kit.
A preculture was used first. Therefore, a single colony was picked from a LB agar plate and transferred in 55 ml LB media with 50 µl Kanamycin and incubated on a shaker at 37°C overnight. To ensure that the culture is not overgrowing, a period of 13 hours (h) should not be surpassed. The bacterial culture was centrifuged for 5000 rpm for 5 minutes the next day, and the supernatant was decanted. The pellet was resuspended in 3 ml S1 buffer by vortexing it. Then, 3 ml S2 buffer was added, vortexed and incubated for 3 minutes. Afterwards, 3 ml S3 buffer was added, the solution was vortexed one more time and centrifuged at 5000 rpm at 4°C for 16 minutes. After centrifugation, the supernatant was filtered. The flow through was loaded on a column that was equilibrated with 1 ml N2 equilibration buffer. The negatively charged plasmid DNA binds to the anion-exchange resin as it flows through the columns by gravity. The column was washed with washing buffer N3 by filling up the whole column twice. The DNA was then eluted with 1 ml elution buffer N5 into a 2 ml Eppendorf cup. In the next step 0.75 ml Isopropanol was added to precipitate the DNA before inverting the tubes ten times and centrifuging at 13000 rpm at 4°C for 30 minutes. In the next step, the supernatant was discarded, the pellet was washed with 1 ml 70% EtOH and centrifugated again at 13000 rpm for ten minutes. The supernatant then was discarded carefully to the last drop by sucking it off with a pipette and the pellet was dried in a drying incubator at 65°C for 10 minutes. In the last step the dry pellet was dissolved in 50 µl sterile water. The concentration of the plasmid solution was measured with the NanoDrop, a photometric spectral analysis system.

2.2.5 Transformation of chemical competent bacteria

This method was used to transfer a plasmid into E.coli DH5α cells to amplify the plasmid amount. 100 µl of E-coli DH5α cells were added to 1 µg plasmid, and the mixture was incubated on ice for 30 minutes. To absorb the plasmid, the cells were heat-shocked at 42°C for 1 minute. After the heat-shock, the cells were transferred gently into the ice without shaking and incubated for 5 minutes. 200 µl of prewarmed LB media was added to the solution and incubated shaking at 37°C for 55 min. In the last step the cell solution was added to 55 ml LB media with 50 µl Kanamycin and was incubated while shaking at 37°C overnight. In the next step the Midi preparation was performed.

2.2.6 Sequencing

Sequencing was progressed to verify that the YAP insert on pEGFP-C3-hYAP1 had the correct sequence, and to further ensure that it was in its right position and the right orientation. Three specific primers were designed to sequence YAP (as can be seen in 2.1.7). Sequencing was performed by Seqlab/Microsynth. For the sequencing reaction, 1.2 µg plasmid DNA and 3 pmol primer solution were combined and filled up to 15 µl with sterile water. Then, the sequencing tube was provided with a bar code and mailed to SeqLab/Microsynth. On the following day, the results (as can be seen in 6.4.1) were downloaded on the SeqLab/Microsynth website.

2.2.7 Proteinbiochemical and immunological assays

2.2.7.1 Preparation of lysates

Lysates were made to extract proteins from cells. About two million cells were transferred into a falcon tube and centrifuged at 300x g for 5 minutes. Afterwards, the media was aspirated, and the cells were resuspended and washed in 5 ml ice-cold PBS. The cells were centrifuged again at 300x g for 5 minutes, and the supernatant was aspirated. The cell pellet was resolved in 1x RIPA Buffer and incubated on ice for 30 minutes. Afterwards, the cells were treated with ultrasound four times for 30 seconds with 30 second breaks on ice in between. Then, the solution was centrifuged at 13000x g for 30 minutes. Finally, the supernatant was pipetted into fresh Eppendorf cups. The protein concentration of the lysates was determined with the Pierce BCA Protein Assay Kit following the manufacturer´s protocol.

2.2.7.2 Loading Western Blot

Sodium dodecyl sulfate polyacrylamide gel electrophoresis (SDS-PAGE) was used to separate the cell lysate by its size. Manufactured gels were placed in the electrode assembly, and the whole module was placed into the running tank. Afterwards, the tank was filled with running buffer. Then, 30 µg protein supplemented with 1x SDS-PAGE Protein Loading Buffer (Reducing) was boiled at 95°C for 5 minutes and loaded on the gel along with 7 µl prestained protein ladder. The gel ran at 200 V for 35 minutes until the dye front reached the bottom of the gel.

2.2.7.3 Blotting and developing Western Blot

To move proteins from the SDS-gel onto a nitrocellulose membrane, western blotting via wet transfer was used. The membrane can be used for protein detection via specific antibodies. All components of the blotting sandwich (filter paper, foam pad, nitrocellulose membrane, SDS-gel) were soaked in Blotting Buffer, and the transfer was proceeded in the blotting chamber with cooling and stir bar on a stirring plate at 100 V for 1.5 hours. The blotting sandwich was disassembled afterwards, and the membrane was stained with Ponceau to ensure that the blotting step worked correctly. Blotting buffer was used to remove the Ponceau afterwards. In the next step, the membrane was incubated in blocking buffer for 1 hour to prevent nonspecific antibody binding. Afterwards, the primary antibodies YAP (1:1000), p-YAP (1:1000) as well as the loading control β-Aktin (1:1000) were given on their specific membranes and were incubated at 4°C overnight. On the next day, the membranes were washed with TBS-T three times for 20 minutes, and the secondary antibodies Peroxidase AffiniPure Donkey Anti-Rabbit (1:10000) and Anti-Mouse (1:10000) were added and incubated for 2 hours on the shaker. Subsequently, membranes were washed again with TBS-T six times for 10 minutes each. As a developing solution, the Western Bright ECL Kit was used following the manufacturer´s protocol. Blots were developed with a Chemidoc imaging system.

2.2.8 Cell culture

All MCC cell lines were kindly provided by Roland Houben and Eva-Maria Sarosi (Department of Dermatology, University Hospital Würzburg, Germany). The MCC cell line PeTa was established at the department of dermatology Mannheim, whereas the cell line WaGa was established from patients at the University Hospital of Würzburg. The MCC cell lines MKL-1, MKL-2 and MS-1 have been described previously (28–30). All cell lines were cultured in suspension in RPMI 1640 media with 10% FCS and 1% PS.

Table 13 MCC cell lines

Cell line	Appearance	Doubling Time	Splitting maximum
WaGa	Single cell suspension	2-3 days	1:4
PeTa	Mid-sized loose spheroids	2-3 days	1:3
MKL-1	Big loose spheroids	2 days	1:4
MKL-2	Medium to big loose spheroids	2-3 days	1:4
MS-1	Medium sized spheroids	3 days	1:3

2.2.8.1 Subculturing

Passaging is a fundamental method for cell cultivation to prevent cell death by avoiding overgrowth. A new culture is produced by transferring cells from the previous culture to new media to achieve a lower density and provide new nutrients as well as avoiding toxic metabolites. All MCC cell lines used are non-adherent cells. In order to build a new passage, 10 ml of the confluent cells were resuspended thoroughly to loosen up the big cell spheroids and were transferred into a new cell culture flask together with 30 ml of new media. It is advised not to remove all of the old media when splitting because the MCC cell lines condition their own media. A cell number of one million cells per ml is the optimum cell density concentration. Hence, all cell lines were split two times a week.

2.2.8.2 Counting cells

To get an accurate number of cells, Luna FL automated cell counter was used. To stain live cells to fluoresce green and dead cells to fluoresce red a specific stain, Acridine Orange (AO)/Propidium Iodid (PI), was used. AO and PI both bind to nucleic acids. AO can permeate viable and dead cells. Binding to ssDNA or RNA results in fluorescing red, and binding to dsDNA results in fluorescing green. PI is not able to permeate viable cells; only dead cells with poor membrane integrity can be entered. Hence, all dead cells are stained with PI and fluorescence red. Cells which are stained with both stains only fluoresce red because the PI signal absorbs the AO signal. To prepare the cells for automated cell counting cell suspension was transferred into a 50 ml falcon tube and centrifuged at 300x g for 5 minutes. The supernatant was aspirated, and the cell pellet was thoroughly resuspended in media to break up big cell spheroids to achieve a better counting result. The amount of media was determined according to the size of the cell pellet. Then, 2 µl of Acridine Orange/ Propidium Iodid Stain was pipetted into one well of a 96-well plate, 18 µl of the cell suspension was added and resuspended. Afterwards, 10 µl of the mixture was loaded on a luna cell counting slide and inserted into the slide port of the Luna

FL automated cell counter. On the screen, an image of the cells appeared, and the focus was adjusted. Luna FL automated cell counter evaluates the total amount of cells, live and dead cells, viability, and the average cell size.

2.2.8.3 Coating with Poly-L-Ornithine

Since all used MCC cell lines are in suspension and partially form cell spheroids, it was difficult to microscope or photograph the cells which was important for further analysis. To singularize the cells and to make them stick to the plastic surface of 6-well plates as well as glass culture slides, the surfaces were coated with Poly-L-Ornithine (PLO). PLO is a synthetic amino acid chain which is positively charged. It is widely used to coat surfaces, to improve adhesion and cell attachment to plastic as well as glass. For establishing the method, 6-well plates were used. However, for the transfection and immunofluorescence experiments, glass culture slides were chosen to enhance the quality of the pictures. For coating 6-well plates, 1 ml of PLO was pipetted on each well. For the glass culture slides, 400 µl of PLO was used for each compartment. By swinging the 6-well plate and the culture slides carefully, it was ensured that the whole surface was coated. The culture dishes were then incubated at 37°C for 1 hour. Afterwards, the supernatant was aspirated, and the surfaces were carefully washed with PBS twice. The newly coated surfaces were used immediately.

2.2.8.4 Transfection with Lipofectamine 3000

Lipofectamine 3000 reagent is a highly efficient transfection reagent designed to transfect DNA into a wide variety of difficult to transfect cell lines with low toxicity.

The day before transfection the cells were split and seeded onto a PLO coated culture slide, containing 180.000 cells per compartment. The media was aspirated on the next day and exchanged with 400 µl of fresh media to keep the conditions as optimal as possible. The lipofectamine transfection reagent was thoroughly vortexed, and 3 µl was diluted in 25 µl of RPMI media without FCS and PS. Moreover, the master mix of DNA was prepared by diluting 1 µg of DNA in 50 µl media without FCS and PS. 2 µl of P3000 reagent was added to the DNA solution and mixed well. 25 µl of the DNA master mix was carefully added to the lipofectamine solution and were incubated at RT for 15 minutes. After the incubation, 50 µl DNA-lipid complex was added carefully drop by drop to each compartment of the culture slide and mixed by gently rocking the slides. Finally, the slides were placed into the CO_2-incubator at 37°C. The best transfection results were achieved after an incubation time of approximately 24 hours.

2.2.8.5 Transfection with K2

In addition to Lipofectamine 3000, the K2 Transfection System was used. The K2 Transfection System consists of the K2 Transfection reagent and the K2 Multiplier. The K2 Transfection reagent is based on strong cationic lipids, and the K2 Multiplier reduces the cells ability to identify foreign nucleic acids and therefore increases the transfection efficiency. The splitting, cell seeding on culture slides and coating process was performed the same as it was with Lipofectamine 3000. To start the transfection process 4 µl K2 Multiplier was added to the cells and incubated at the CO_2-incubator at 37°C for 2 hours. In the meantime, 26 µl media without FCS and PS and 10 µl K2 Transfection reagent were pipetted into an Eppendorf cup and were vortexed thoroughly. Then, 3 µg DNA was diluted in 26 µl media without FCS and PS. To prepare the lipoplex 29 µl of DNA dilution was added to the cup of diluted K2 transfection reagent and incubated at room temperature for 15 minutes. Afterwards, 60 µl of the lipoplex was dispensed carefully onto the cells which were then incubated in the CO_2-incubator for approximately 24 hours to obtain optimal results.

2.2.8.6 Conservation of mammalian cells

For conservation purposes the cells were stored for two weeks at -80°C and later transferred to liquid nitrogen. Therefore, one million cells were counted, washed in PBS twice and were given into a cryogenic tube with 1 ml of freezing media. The freezing media consists of 900 µl FCS as well as 100 µl DMSO to prevent the mixture of building ice crystals which would cause cell death. Afterwards, the cryogenic tubes were placed at -80°C.

2.2.9 Immunofluorescence

To visualize expression and localisation of certain proteins, indirect immunofluorescence was used. A specific primary antibody binds to a protein that is recognized by a secondary antibody labelled with fluorochrome. The fluorochrome can be detected with a fluorescence microscope supplied with filters specific for the emission wavelength of the fluorochrome. Media was removed carefully 24 hours after transfection of the cells, which were then washed with PBS twice. The cells were then fixed by using prewarmed 4% paraformaldehyde in PBS (pH 7) for 10 minutes at RT. Afterwards, the fixative was aspirated, and the cells were washed with PBS three times for 5 minutes while shaking. To avoid unspecific binding, the cells were blocked with blocking buffer at RT while shaking for one hour. The primary antibody Ki-67 was prepared by diluting in Antibody Dilution Buffer (1:800). Ki-67 is a cellular marker and nuclear protein that is associated with cell proliferation. Ki-67 is absent in resting cells but can be detected in all active phases of the cell cycle, which makes it an ideal marker for cell division and consequently proliferation. The blocking buffer was aspirated, and the diluted primary antibody was added to the cells. The cells were stained overnight at 4°C. On the next day, the primary antibody was aspirated, and the cells were washed with PBS three times for 5 minutes each. Ki-67 is made visible by linking it to a second antibody, Alexa Flour 594, which fluoresces red. The secondary antibody Alexa Flour 594 was diluted in Antibody Dilution Buffer (1:500) and added to the cells. The cells were incubated at RT in the dark for one hour while shaking. Afterwards, the antibody dilution was rinsed off with PBS three times for 5 minutes each while protecting from light. The slides were mounted in the dark with Mounting Media with DAPI a nuclear stain and analysed under the fluorescence microscope directly.

2.2.10 Statistics

Statistical analyses were performed using the statistical software GraphPad Prism 6. A two-tailed Student´s unpaired *t*-test was used for statistical analysis. A p-value of < 0.05 was regarded as statistically significant.

3 Results

3.1 YAP expression in Merkel cell carcinoma

To test whether the Hippo signaling pathway plays a role in the pathogenesis of MCC, 47 Merkel cell carcinoma tissue samples were immunohistochemically stained with total-YAP antibody (Figure (Fig.) 3, two middle columns in 2.5x A´ - D´ and 20x magnification A´´ - D´´). Human testis tissue served as a positive control (Fig.2).

The immunohistochemical staining with the specific monoclonal antibody total-YAP (Fig. 3 two middle columns A´ - D´´) showed positive staining of the epidermis, the epithelium of sweat and sebaceous glands, blood vessels and peritumoral lymphocytes in all samples. However, there was no expression of YAP in carcinoma cells of all 47 MCC tissue samples.

In addition, two further stainings were performed. Firstly, the HE staining (Fig.3, first column A-D), which serves as an overview-staining. Secondly, another immunohistochemical staining with the specific monoclonal antibody CK20 (Fig.3, last column A´´´ - D´´´) was carried out.

CK20 serves as a marker to verify the diagnosis of Merkel cell carcinoma. The immunohistochemical staining with CK20 shows diffuse cytoplasmic staining of the tumor cells. CK20 was expressed in the tumor tissues used in this study (Fig.3. last column A´´´ - D´´´).

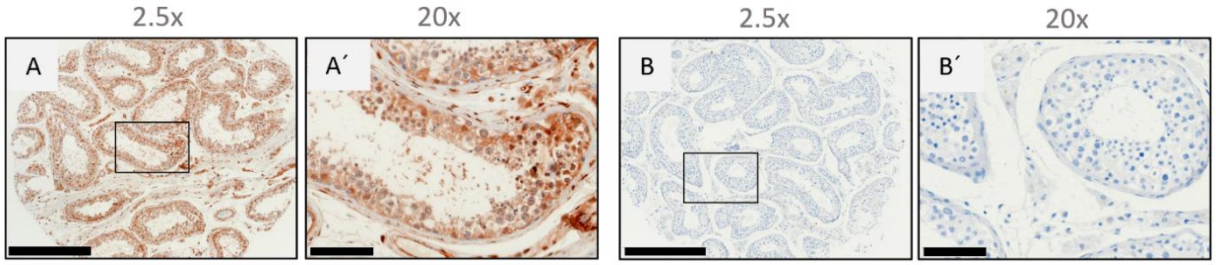

Figure 2 YAP expression in human testis

A-A`** Human testis tissue as positive control, **B-B` Human testis tissue as negative control, stained without primary antibody, in 2.5x and 20x magnification. Black scale bar in A and B: 1mm and A´ and B´: 100 µm.

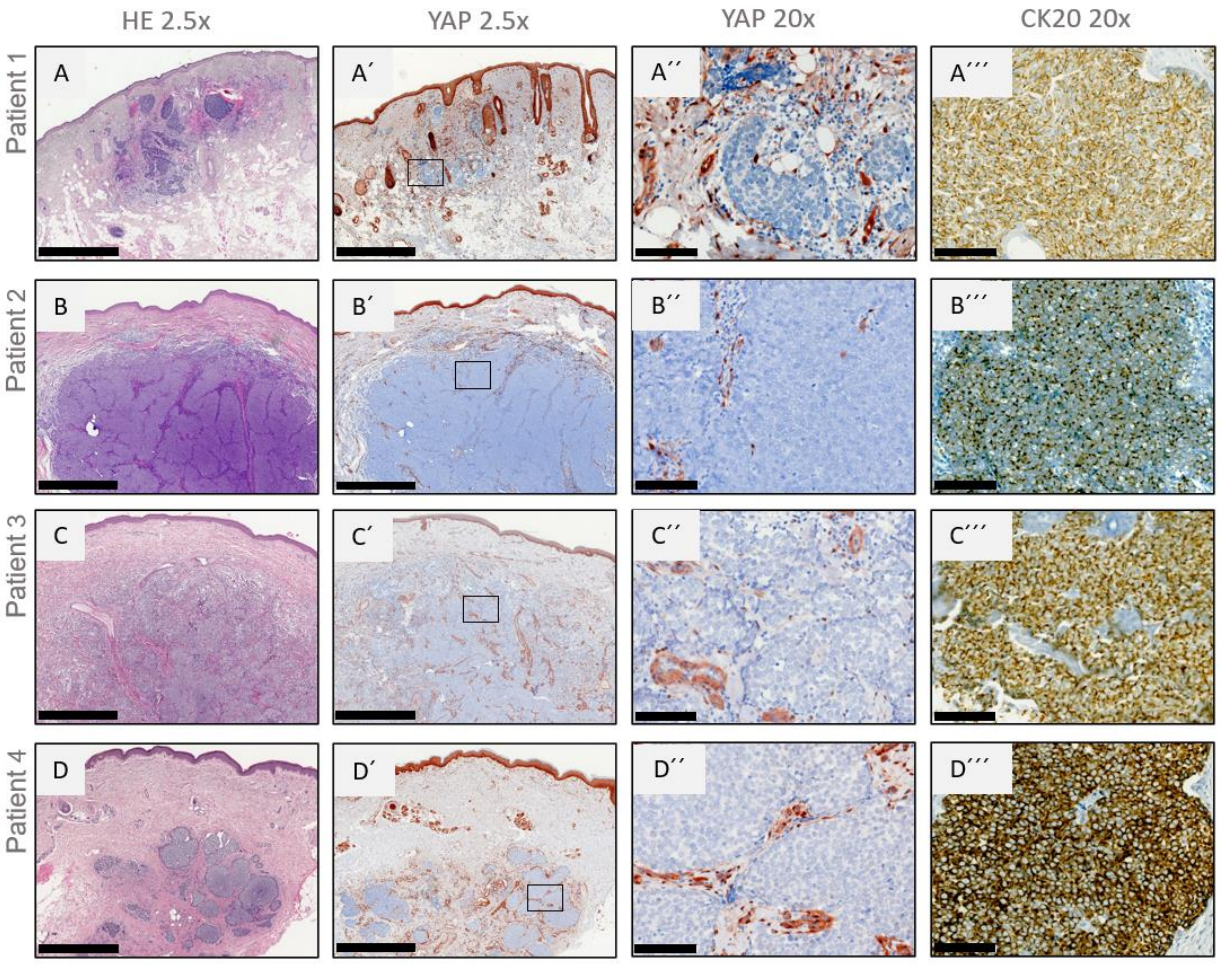

Figure 3 Immunohistochemistry of five MCC patient biopsies

Hematoxylin and eosin staining (first column, **A-D**). Immunohistochemical staining of YAP (second and third column**, A´- D´´**) and CK20 (last column, **A´´´- D´´´**) on Merkel cell carcinoma. Black scale bar in first two columns: 1 mm, in last two columns 100 µm. The Merkel cell carcinoma cells show no expression of YAP. CK20 is strongly expressed in all tumors.

3.2 Western Blot indicates no YAP and p-YAP expression in MCC cell lines

Western blot analysis was used to detect β-Actin, YAP and p-YAP in five different MCC cell lines WaGa, PeTa, MKL-1, MKL-2 and MS-1. β-Actin was used as a loading control and shows that all samples were loaded with the same amount of protein (Fig. 4, bottom). It was examined whether YAP and its phosphorylated status p-YAP is expressed in any of the cell lines, as YAP (Fig.4, top row), as well as p-YAP (Fig.4 middle row), are taken as a measure of activity of the Hippo signalling pathway. The fast-growing and very robust melanoma cell line A375 was used as a positive control. Both YAP and p-YAP are expressed in the melanoma cell line (Fig. 4, two strong bands on the very right). However, none of the Merkel cell carcinoma cell lines shows any expression of YAP or p-YAP.

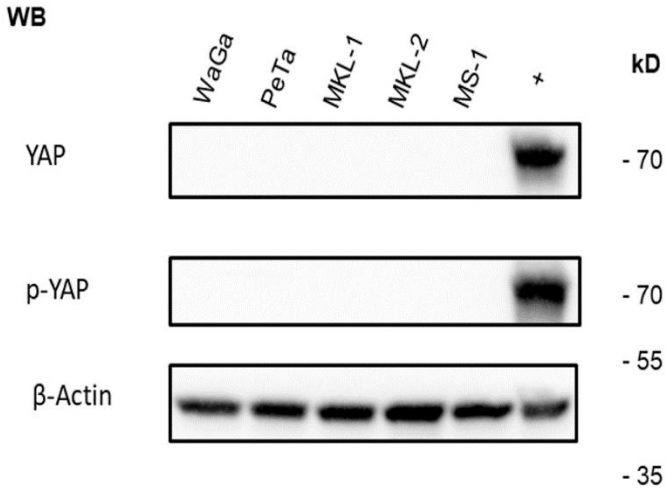

Figure 4 Western Blot analysis of YAP and p-YAP

Western Blot analysis of expression of YAP and p-YAP in Merkel cell cancer cell lines. YAP as well as p-YAP is expressed in the melanoma cell line A375, used as the positive control (on the very right marked with +). Consistent with the immunohistochemistry results, there is no expression of YAP or p-YAP in the MCC cell lines.
β-Actin was used as a loading control (bottom).

3.3 Coating with Poly-L-Ornithine leads to best adherence results

All five MCC cell lines used in this study were challenging to work with, as they are in suspension, and their cells stick together and form spheroids. However, for further analysis (as can be seen in 3.4 and 3.5) it was crucial to achieve greater clarity by singularizing the cells and making them adhere to the culture slide surfaces to microscope, photograph, stain, transfect and count the cells. Different experimental setups were chosen to evaluate which cell lines and coating materials achieved optimum conditions and requirements. As a coating material, PLO, Collagen 1 and no coating were compared as well as all MCC cell lines, WaGa, PeTa, MKL-1, MKL-2 and MS-1. Best results were achieved by using 1 ml undiluted PLO for coating 6-well plates and 400 µl for each compartment of the glass culture slides. Best adherence was achieved by incubating the culture dishes at 37°C for 1 hour, seeding the cells immediately afterwards and incubating the coated culture slides overnight. Visual control under the microscope showed that the experimental setups without coating were unsuccessful as almost no cells were left on the surfaces. Coating with Collagen 1 diluted 1:1 with PBS, was only successful with the WaGa cell line (60% of the cells adhered to the culture slides). The best results by far were achieved with PLO and the cell lines WaGa and PeTa where 80% of the initially seeded cells were attached to the surfaces of the culture dishes. MKL-1, MKL-2 and MS-1 had a poor outcome so that further experiments with these three cell lines were abandoned.

3.4 Best Transfection Efficiency with Lipofectamine 3000

Since immunohistochemistry and Western Blot analysis showed no expression of YAP in the MCCs, a plasmid DNA with pEGFP-C3-hYAP1 (plasmid sequence map can be seen in further supplementary material 6.4.2) was transfected into the MCC cells. The empty pEGFP-C3 plasmid (plasmid sequence map can also be seen in 6.4.2) served as a negative control. The transfection was performed to examine if YAP expression affects the proliferation of MCC cells.

Lipofectamine 3000 and K2 were tested under a wide range of different experimental conditions to obtain the best transfection efficiency results. Only the cell lines WaGa and PeTa were tested further, as MKL-1, MKL-2 and MS-1 showed no successful results.

Transfection efficiency was observed 6, 12, 24 and 48 hours after transfection. In all test setups with K2 as well as Lipofectamine 3000, the transfection efficiency was the highest after 24 hours. Consequently, all results were evaluated 24 hours after transfection.

Another crucial factor was the amount of Merkel cell carcinoma cells per compartment as well as their cell division status. By considering the proliferation stage of the cells, coverage of the cell growth area of 90-100% is ideal. As healthy and well proliferating cells are transfected the easiest, the best results were achieved with K2 as well as Lipofectamine 3000 by splitting the cells one day before and seeding 180.000 cells per PLO coated culture slide compartment. In this state of growth, the cells are proliferating the most which ensures the insertion of DNA into the nucleus, through break-up and rebuilding of the membrane during the splitting process of the cells.

Comparing Lipofectamine 3000 to K2 on their transfection performance, a 30% transfection efficiency with Lipofectamine 3000 and 20% transfection efficiency with K2 under the same conditions could be observed. However, the toxicity of K2 was higher than of Lipofectamine 3000.

K2 transfection required a more laborious and time-consuming preparation than Lipofectamine 3000, and K2 showed higher toxicity. This led to the decision to conduct further experiments with Lipofectamine 3000 only.

A crucial factor for an optimal transfection with Lipofectamine 3000 was the exact concentration of lipofectamine transfection reagent, P3000 reagent, DNA amount and its concentration, as every cell line has its own specific optimal range. The following protocol was developed to achieve best results: 3 µl lipofectamine transfection reagent diluted in 25 µl of RPMI media without FCS and PS was used. 1µg of DNA was diluted in 50 µl of the same media. 25 µl of the DNA master mix was added to the lipofectamine solution. After incubating the mix for 15 min at RT, 50 µl DNA-lipid complex was added to each compartment and was placed in a CO_2-incubator at 37°C for 24 hours. The cells were assessed with a fluorescence microscope the next day.

3.5 Immunofluorescence shows no significant difference between cells with and without YAP in proliferation

After elaborating an effective process to transfect the EGFP-hYAP1 and the EGFP plasmids, further immunofluorescence experiments were executed to see if implementing YAP into the MCC cells has an influence on their cell proliferation compared to cells transfected with the empty EGFP-vector. WaGa and PeTa cells were fixed and the primary antibody Ki-67 was added. Ki-67 is a marker for cell division and, therefore, proliferation.

A mounting media with DAPI was used for nuclear staining which let all cell nuclei appear blue under the fluorescence microscope (Fig.5-7). Successful transfection of the cells presented green fluorescing cells, as both plasmids used in this study had EGFP (plasmid maps are shown in further supplementary material 6.4.2).

The melanoma cell line A375 was used as a positive control. The experiment was performed three times under precisely the same circumstances. In each biological replicate (B1, B2 and B3), around 200 green fluorescing cells of both cell lines and plasmids, were randomly picked and it was counted whether they fluoresced red and thus were Ki-67 positive (exact numbers are shown in further supplementary material 6.4.3).

The MCC cell line WaGa transfected with the control plasmid, pEGFP-C3, showed 69.81 ± 13.56% of Ki-67 positive cells. After transfection of the YAP-plasmid, pEGFP-C3-hYAP1, 95.57 ± 1.83% were Ki-67 positive. In summary, the cells transfected with EGFP-C3-hYAP1 and its empty vector EGFP-C3 showed no significant difference in the expression of Ki-67 as tested with unpaired *t*-test ($p=0.133$) as seen in Figure 8. In the PeTa cell line transfection of the empty vector, EGFP-C3 resulted in 58.39 ± 11.09% of Ki-67 positive cells. Cells containing YAP after transfection of EGFP-C3-hYAP1 were Ki-67 positive in 79.02 ± 3.30%. The difference was, as well, statistically not significant ($p=0.149$).

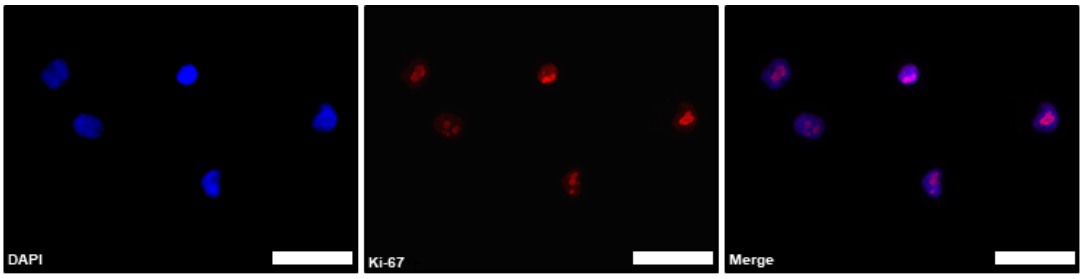

Figure 5 Immunofluorescence Positive control

The melanoma cell line A375 was used as a positive control in the immunofluorescence experiments. Nuclear staining (DAPI, blue, first picture), staining with proliferation marker Ki-67 (red, second picture) and in combination (merge, last picture). White scale bar: 50 µm.

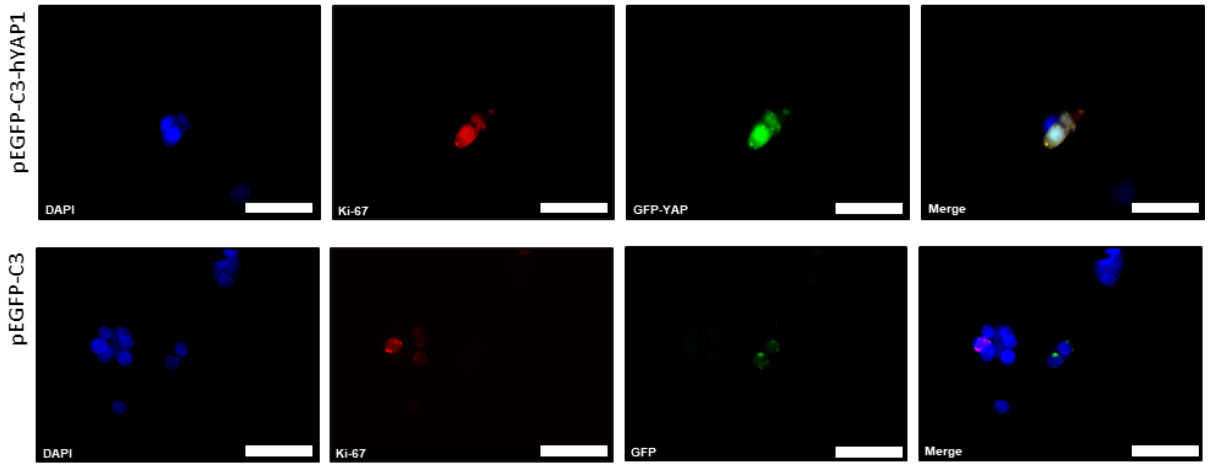

Figure 6 Immunofluorescence of WaGa

MCC cell line WaGa transfected with plasmid pEGFP-C3-hYAP1 (green, top row) and its equivalent empty vector pEGFP-C3 (green, bottom row). Afterwards cells were stained with Ki-67 (red, second column) antibody as well as nuclear staining DAPI (blue, first column). DAPI, GFP, GFP-YAP and Ki-67 in combination (merge, last column).
White scale bar is 50 µm.
95,94% of cells with transfected YAP showed Ki-67 staining and 69,61% of cells transfected with the empty vector showed Ki-67.

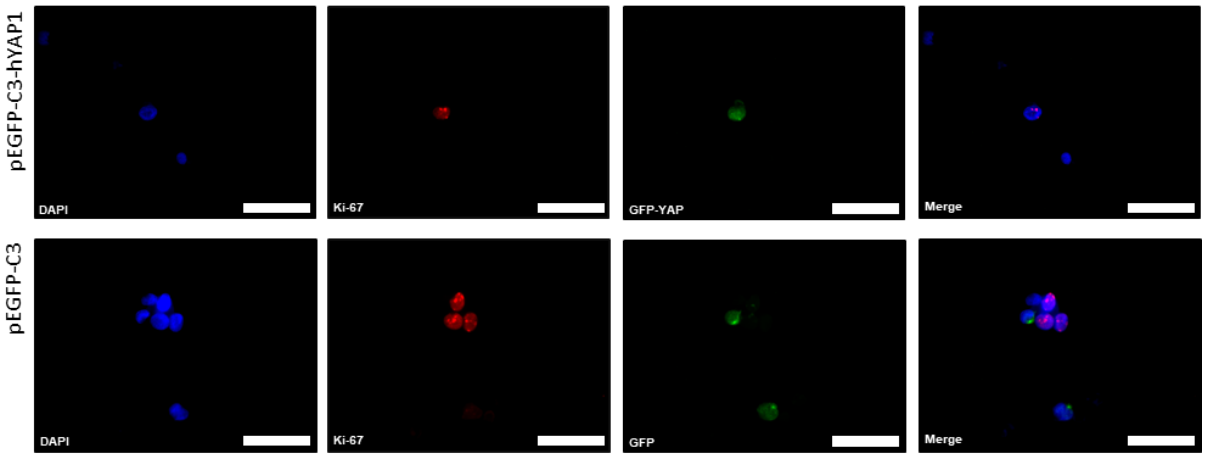

Figure 7 Immunofluorescence of PeTa

MCC cell line PeTa was transfected and stained in the same way WaGa was. White scale bar is 50 µm. Nuclear staining DAPI (blue, first column), Ki-67 antibody (red second column), transfected cells with GFP and GFP-YAP (green, third column) and the combination of all three (merge, last column).
78,84% MCC cells transfected with YAP showed Ki-67 staining and 61,99% of cells transfected with the empty vector showed Ki-67 staining.

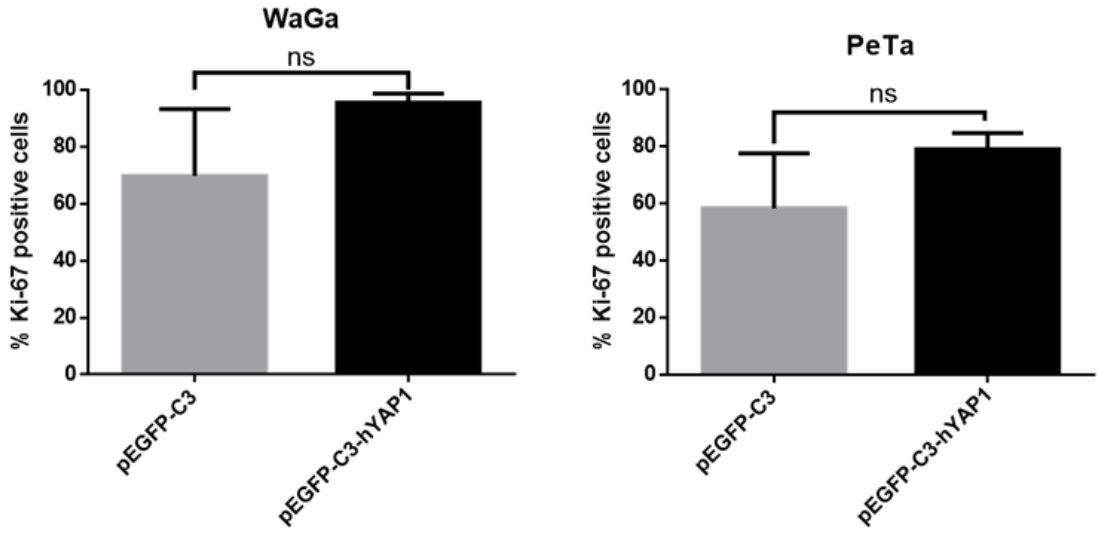

Figure 8 Ki-67 positive cells after transfection with YAP and an empty vector

A transfection with pEGFP-C3-hYAP1 as well as pEGFP-C3 was performed with the cell lines PeTa and WaGa. WaGa as well as PeTa showed no significant difference between cells with YAP or with the empty vector (tested with unpaired *t*-test p=0.1329 and p=0.1491, respectively).

4 Discussion

4.1 Immunohistochemistry

YAP, as the major effector of the Hippo signaling pathway, has been the subject of numerous studies on carcinoma development in recent years. These studies have shown that the dysregulation of the Hippo signaling pathway is playing a crucial role in the development of colorectal cancer, liver cancer, ovarian cancer and lung tumor progression and metastasis (31–34). In addition, several skin cancers are affected by the oncoprotein YAP. Studies by Debaugnies et al., Jia et al. and Quan et al. examined the presence of YAP in basal cell carcinoma (25,35,36). Furthermore, several studies show a clear presence of YAP activity in melanoma (26,37–39). In 2019, Dong et al. confirmed YAP as a promising target for squamous cell carcinoma (40). Squamous cell carcinoma is common in patients with Merkel cell carcinoma. Both tumors are associated, and a common carcinogenetic influence for squamous and Merkel cell carcinomas of the skin is suspected (41,42).

These important findings in tumor research suggest that the Merkel cell carcinoma could also be influenced by the Hippo signaling pathway. To the current state of knowledge, this is the first study investigating the connection between Merkel cell carcinoma and the Hippo signaling pathway.

Unexpectedly, none of the 47 immunohistochemically stained tissue samples of Merkel cell carcinoma showed any expression of YAP. It seems that the Hippo signaling pathway is not activated in the tumor. This implies that other pathways control the tumorigenesis of Merkel cell carcinoma.

In this study, a relatively large number of 47 tissue samples of the rare MCC was used. This factor distinguishes this study from other publications and underlines its significance, as a majority of studies investigating MCC in immunohistochemistry use much smaller sample sizes (41,43–45).

4.2 Western Blot

In addition to the immunohistochemical experiments, the method of western blotting was performed to detect the expression of YAP and its phosphorylated state p-YAP in five different MCC cell lines. Consistent with the immunohistochemistry analysis, YAP expression was absent in all Merkel cell carcinoma cell lines. This shows that, unlike numerous other tumors, (24,25,46,47) the Hippo signaling pathway is not involved in the development of MCC. At this point, there are no publications investigating YAP and the role of Hippo signaling pathway in MCC. As the pathogenesis and molecular basis of Merkel cell carcinoma are not yet entirely understood, further studies are needed to contribute to a better understanding of the tumorigenesis of Merkel cell carcinoma.

4.3 Coating

A widespread problem in cell culture experiments, that also presented a technical limitation for the transfection experiment used in this study, is the insufficient cell-surface adhesion of MCC cell lines to the surface of tissue culture slides. In this investigation, best adherence results were achieved by using PLO in combination with the cell lines WaGa and PeTa. Although all MCC cell lines were challenging to handle, WaGa, which grows in a single cell suspension, and PeTa, that grows in big loose spheroids, had the best outcome (10,48). The other three cell lines MKL-1, MKL-2 and MS-1 grow in big spheroids, and their cells stick together more tightly. A possible explanation of why these cell lines are more difficult to adhere to a surface could be the fact, that these cells are difficult to reach by PLO or that the cell-cell-adherence in big spheroids is stronger.

Daily et al. found that the phenotypic similarity of the WaGa cell line is very close to the native tumor of Merkel cell carcinoma (49). Thus, experiments with this cell line can be considered representative for MCC and therefore more significant.

Zhao et al. showed that the Hippo pathway kinases Lats1/2 are activated by cell detachment from the extracellular matrix which leads to YAP phosphorylation and inhibition (50). Treating the cells with PLO causes detachment of the cells. This could have had a possible influence on YAP and the Hippo signalling pathway and therefore could have affected the transfection experiments.

PLO is an established and widely used reagent for cell-surface adhesion. A study about the effects of coating materials on prostate cancer cell adherence showed that PLO reduced cell mobility and significantly affected cell viability (51). Moreover, Harnett et al. observed the surface energy of different materials coated with adhesion molecules and concluded, that PLO produces a monopolar basic surface. Depending on the underlying substrates they were coated on, it could provide a hydrophobic or hydrophilic surface (52). In conclusion, surface coating has a strong impact on cells and therefore has the potential to falsify transfection results. A possible solution to this problem could be adherent MCC cell lines as described by Leonard et al. (53,54). These cell lines could pose a good alternative for future studies.

4.4 Transfection

In this study, a plasmid DNA with EGFP-C3-hYAP1 was transfected into MCC cells using the two different transfection systems K2 and Lipofectamine 3000. Best results were achieved using Lipofectamine 3000 with a transfection efficiency of 30% compared to a transfection efficiency of 20% of the K2 transfection system.

A study by Shi et al., that compared three different transfection reagents (FuGENE 6, Lipofectamine 2000 and Lipofectamine 3000) showed that Lipofectamine 3000 had the highest transfection efficiency (55). Another study, comparing five different commonly used transfection reagents, reported the best transfection results in FuGENE, RNAiMAX and Lipofectamine 3000. However, the transfection efficacy seems to have a positive correlation with the toxicity of transfection reagents. Therefore, Wang et al. suggest using RNAiMAX when lower toxicity is required (56). In the present study, Lipofectamine 3000 also showed the highest transfection efficiency. Another alternative could be the transfection reagent Turbofect. A lower cytotoxicity of Turbofect compared to Lipofectamine 3000 was reported by Rahimi et al. Furthermore, they found that a non-adherent cell line transfected with pEGFP-N1 showed better results with Turbofect than with Lipofectamine 3000 (57). These results can be compared to the findings of the present study, also using a non-adherent cell line transfected with a similar plasmid structure. For further studies, the use of RNAiMAX or Turbofect could possibly lead to a higher transfection efficiency and a lower cytotoxicity.

In this study, the best outcome in transfection efficiency was achieved by doubling the amount of plasmid DNA and transfection reagent. However, it was found that much higher or lower concentration of the recommended amount did not lead to a better result. A similar effect was reported by Gonzalez et al. who transfected mesenchymal stem cells using Xfect, Turbofect and Lipofectamine 3000. They concluded that cell viability did not diminish, and transfection efficiency enhanced by increasing the volume of transfection agent, the plasmid DNA mass or both. Efficiency improved by 70% by doubling the quantities recommended by the manufacturer (58).

4.5 Immunofluorescence

MCC cells were transfected with the YAP vector EGFP-C3-hYAP1 and the empty vector EGFP-C3 to investigate the influence of YAP on cell proliferation. The marker used for cell proliferation was Ki-67. The cell line WaGa transfected with the YAP-plasmid, and the control plasmid showed no significant difference in the expression of Ki-67 as tested with the unpaired *t*-test (p=0.133). The difference in the PeTa cell line was statistically not significant either (p=0.149). These data suggest that the Hippo signaling pathway is not involved in the development of MCC progression.

So far, numerous studies were carried out to contribute to a better understanding of the pathogenesis and molecular basis of Merkel cell carcinoma.

Studies by Houben et al., Popp et al. and van Gele et al. found that a p53 mutation was rare in the majority of MCC investigated (10,41,59). A study by Goh et al. showed only a few mutations in MCPyV-positive MCC. However, a high mutation burden in MCPyV-negative MCC was found (60). These results suggest that the use of immunotherapies for virus-negative MCCs could be a possible solution in the fight against the aggressive tumor.

The Wnt-signaling pathway was examined by Liu et al. In only one of twelve cases of MCC, nuclear accumulation of β-catenin was observed and they thus concluded that the Wnt-signaling pathway does not play an important role in the tumorigenesis of MCC (45). A recently published study by Weeraratna et al. underlines these results by showing a lack of Wnt5A expression in MCC (61).

The oncogenic pathway in MCC most studied is the mitogen-activated protein (MAP) kinase signaling pathway. Several studies have found an expression of the potential activator of the MAP kinase pathway, c-kit, in MCC (62–65). Swick et al. reported eight of nine MCC tissue samples positive for c-kit in immunohistochemical staining, however, no mutations were found (66). In 2013, the same study group confirmed these results and concluded that the absence of activating mutations in the tyrosine kinases makes c-kit an improbable candidate of MCC oncogenesis (67).

The analysis of the oncogenes Ha-ras, Ki-ras, N-ras and B-raf did not show any mutation in MCC (41,68,69). Houben et al. revealed that the MAP-kinase pathway

was silenced in 42 out of 44 MCC samples and concluded that the MAP-kinase signaling pathway is inactive in Merkel cell carcinoma (69).

Understanding the pathogenesis of MCC is vital in the development of effective therapies of the tumor. A potential point of attack in MCC treatment could be the anti-apoptotic molecule bcl-2, which was expressed in about three-quarter of MCC in three independent studies (70–72). A recent study by Liu et al. suggests a bcl-2 inhibition in combination with DNA damage-induced apoptosis as a new therapeutic strategy for MCPyV-positive MCCs (73).

Another novel therapeutic target in MCC is the PI3K/AKT pathway. A study by Hafner et al. showed high levels of AKT phosphorylation in MCC. Furthermore, all cell lines were sensitive towards a PI3K inhibitor. These findings lead to the conclusion that the PI3K/AKT pathway is active in a majority of MCC, which makes it an interesting aim for future therapies (74).

The Merkel cell polyomavirus, identified in 2008, should also be considered a possible target in developing a treatment for MCC (9). A study by Starrett et al. shows the strong effect that MCPyV has on viral MCC tumorigenesis and that the virus is capable of hijacking cellular processes and showing dominant control of the genome of virus-positive MCCs (75). A better understanding of the distinct mutagenic mechanisms in viral and nonviral MCC has a significance for the effective treatment of these tumors, and therefore, further studies are needed.

Since MCC is a highly aggressive tumor with poor prognosis and still very limited therapeutic options, the presented study investigating the influence of the Hippo signaling pathway in MCC is not yet the final endpoint on the long and difficult process of finding a suitable cure for MCC. However, it does take us a big step forward in gaining a better understanding of the tumorigenesis of MCC.

5 Summary

Merkel cell carcinoma (MCC) is a rare and highly aggressive neuroendocrine skin cancer. The understanding of the molecular pathogenesis of MCC is still limited. To assess the relevance of the Hippo signaling pathway in MCC, the presence of the major effector of the pathway, the yes-associated protein (YAP) was investigated. An immunohistochemical analysis of 47 tumor tissues and a Western Blot analysis of 5 MCC cell lines were performed. All MCC samples and cell lines showed no expression of YAP. For immunofluorescence experiments, two MCC cell lines in suspension were adhered to culture slides, using PLO. The cells were then transfected with a plasmid DNA containing YAP and its empty vector, as a negative control. The transfection was performed to examine if YAP expression affects the proliferation of MCC cells. Ki-67 served as a marker for cell proliferation and was analysed in an immunofluorescence experiment. Both cell lines transfected with the YAP-plasmid, and its empty vector showed no significant differences in the expression of Ki-67. In summary, these data demonstrate that the Hippo signaling pathway is not involved in the development of the MCC progression. Further immunological and molecular studies are necessary for a deeper understanding of the tumorigenesis of the Merkel cell carcinoma.

6 Supplementary data

6.1 Abbreviations

AO:	Acridine Orange
B:	biological replicate
BSA:	Bovinum Serum Albuminum
CK20:	Cytokeratin 20
ddH_2O:	distilled water
DMSO:	Dimethylsulfoxide
DPBS:	Dulbecco Phosphate Buffered Saline
DTT:	Dithiothreitol
E.coli:	Escherichia coli
EtOH:	Ethanol
FCS:	Feral cow serum
Fig.:	Figure
HE:	Hematoxylin and Eosin staining
HCl:	Hydrochloric acid
H_2O_2:	Hydrogen peroxide
IF:	Immunofluorescence
IHC:	Immunohistochemistry
KCl:	Potassium chloride
kD:	kilodalton
LATS:	large tumor suppressor
mAb:	monoclonal Antibody
MAP:	mitogen-activated protein

materialno:	material number
MCC:	Merkel cell carcinoma
MCPyV:	Merkel cell polyoma virus
min:	minutes
MST:	mammalian STE20-like protein kinase
NaCl:	Sodium chloride
NaOH:	Sodium hydroxide
PBS:	Phosphate buffered saline
PI:	Propidium Iodide
PLO:	Poly-L-Ornithine
PS:	Penicillin-Streptomycin
p-YAP:	phospho-Yes associated protein
RIPA:	Radioimmunoprecipitation assay
RT:	room temperature
sec:	seconds
Ser/Thr:	serine-threonine
Seq:	Sequence
SDS:	Sodium dodecyl sulfate
SDS-PAGE:	Sodium dodecyl sulfate polyacrylamide gel electrophoresis
TBS:	Tris buffered saline
TEAD:	TEA domain family
WB:	Western Blot
WWTR1:	WW domain-containing transcription regulator protein 1
YAP:	Yes associated protein

6.2 Table of figures

6.3 Table of tables

6.4 Further supplementary material

6.4.1 Sequencing Results

Sequence of YAP1 Seq.1 neu

Economy Run (Tube)

40920863 3344101

YAP Seq1-NEW

NGGATCCCCGCATATGGATCCCGGGCAGCAGCCGCCGCCTCAACCGGCCCCCCAGGGCCAAGGGCAGCCGCCTTC
GCAGCCCCCGCAGGGGCAGGGCCCGCCGTCCGGACCCGGGCAACCGGCACCCGCGGCGACCCAGGCGGCGCCGCA
GGCACCCCCCGCCGGGCATCAGATCGTGCACGTCCGCGGGGACTCGGAGACCGACCTGGAGGCGCTCTTCAACGC
CGTCATGAACCCCAAGACGGCCAACGTGCCCCAGACCGTGCCCATGAGGCTCCGGAAGCTGCCCGACTCCTTCTT
CAAGCCGCCGGAGCCCAAATCCCACTCCCGACAGGCCAGTACTGATGCAGGCACTGCAGGAGCCCTGACTCCACA
GCATGTTCGAGCTCATTCCTCTCCAGCTTCTCTGCAGTTGGGAGCTGTTTCTCCTGGGACACTGACCCCCACTGG
AGTAGTCTCTGGCCCAGCAGCTACACCCACAGCTCAGCATCTTCGACAGTCTTCTTTTGAGATACCTGATGATGT
ACCTCTGCCAGCAGGTTGGGAGATGGCAAAGACATCTTCTGGTCAGAGATACTTCTTAAATCACATCGATCAGAC
AACAACATGGCAGGACCCCAGGAAGGCCATGCTGTCCCAGATGAACGTCACAGCCCCCACCAGTCCACCAGTGCA
GCAGAATATGATGAACTCGGCTTCAGCCATGAACCAGAGAATCAGTCAGAGTGCTCCAGTGAAACAGCCACCACC
CCTGGCTCCCCAGAGCCCACAGGGAGGCGTCATGGGTGGCAGCAACTCCAACCAGCAGCAACAGATGCGACTGCA
GCAACTGCAGATGGAGAAGGAGAGGCTGCGGCTGAAACAGCAAGAACTGCTTCGGCAGGTGAGGCCACAGGAGTT
AGCCCTGCGTAGCCAGTTACCAACACTGGAGCAGGATGGTGGGACTCAAAATCCAGTGTCTTCTCCCGGGATGTC
TCAGGAATTGAGAACAATGACGACCAATAGCTCAGATCCTTTCCTTAACAGTGGCACCTATCACTCTCGAGATGA
GAGTACAGACAGTGGACTAAGCATGAGCAGCTACAGTGTCCCTCGAACCCCAGATGACTTCCTGAACAGKGKGGA
TGAAATGGA

Sequence of YAP1 Seq.2

BC Economy Run

40856585 3344092

YAP Seq2

CCACTGGAGTAGTCTCTGGCCCAGCAGCTACACCCACAGCTCAGCATCTTCGACAGTCTTCTTTTGAGATACCTG
ATGATGTACCTCTGCCAGCAGGTTGGGAGATGGCAAAGACATCTTCTGGTCAGAGATACTTCTTAAATCACATCG
ATCAGACAACAACATGGCAGGACCCCAGGAAGGCCATGCTGTCCCAGATGAACGTCACAGCCCCCACCAGTCCAC
CAGTGCAGCAGAATATGATGAACTCGGCTTCAGCCATGAACCAGAGAATCAGTCAGAGTGCTCCAGTGAAACAGC
CACCACCCCTGGCTCCCCAGAGCCCACAGGGAGGCGTCATGGGTGGCAGCAACTCCAACCAGCAGCAACAGATGC
GACTGCAGCAACTGCAGATGGAGAAGGAGAGGCTGCGGCTGAAACAGCAAGAACTGCTTCGGCAGGTGAGGCCAC
AGGAGTTAGCCCTGCGTAGCCAGTTACCAACACTGGAGCAGGATGGTGGGACTCAAAATCCAGTGTCTTCTCCCG
GGATGTCTCAGGAATTGAGAACAATGACGACCAATAGCTCAGATCCTTTCCTTAACAGTGGCACCTATCACTCTC
GAGATGAGAGTACAGACAGTGGACTAAGCATGAGCAGCTACAGTGTCCCTCGAACCCCAGATGACTTCCTGAACA
GTGTGGATGAGATGGATACAGGTGATACTATCAACCAAAGCACCCTGCCCTCACAGCAGAACCGTTTCCCAGACT
ACCTTGAAGCCATTCCTGGGACAAATGTGGACCTTGGAACACTGGAAGGAGATGGAATGAACATAGAAGGAGAGG
AGCTGATGCCAAGTCTGCAGGAAGCTTTGAGTTCTGACATCCTTAATGACATGGAGTCTGTTTTGGCTGCCACCA
AGCTAGATAAAGAAAGCTTTCTTACATGGTTATAGAGCCCTCAGGCAGACTGAATTCAGATCCACCGGATCTAGA
TAACTGATCATAATCAGCCATACCACATTTGTAGAGGTTTTACTTGCTTTAAAAAACCTCCCACACCTCCCCCTG
AACCTGAAACATAAAATGAATGCAATTGTTGTTGTTAACTTGTTTATTGCAGCTTATAATGGTTACAAATAAAGC
CATAGCATCMCAAATTTCMCAAATAAAGCATTTTTTTCCTGCATTCNAR

Sequence of YAP1 Seq.3

BC Economy Run

40856586 3344093

YAP Seq3

GCGACYGCAGCACTGCAGATGGAGAAGGAGAGGCTGCGGCTGAAACAGCAAGAACTGCTTCGGCAGGTGAGGCCA
CAGGAGTTAGCCCTGCGTAGCCAGTTACCAACACTGGAGCAGGATGGTGGGACTCAAAATCCAGTGTCTTCTCCC
GGGATGTCTCAGGAATTGAGAACAATGACGACCAATAGCTCAGATCCTTTCCTTAACAGTGGCACCTATCACTCT
CGAGATGAGAGTACAGACAGTGGACTAAGCATGAGCAGCTACAGTGTCCCTCGAACCCCAGATGACTTCCTGAAC
AGTGTGGATGAGATGGATACAGGTGATACTATCAACCAAAGCACCCTGCCCTCACAGCAGAACCGTTTCCCAGAC
TACCTTGAAGCCATTCCTGGGACAAATGTGGACCTTGGAACACTGGAAGGAGATGGAATGAACATAGAAGGAGAG
GAGCTGATGCCAAGTCTGCAGGAAGCTTTGAGTTCTGACATCCTTAATGACATGGAGTCTGTTTTGGCTGCCACC
AAGCTAGATAAAGAAAGCTTTCTTACATGGTTATAGAGCCCTCAGGCAGACTGAATTCAGATCCACCGGATCTAG
ATAACTGATCATAATCAGCCATACCACATTTGTAGAGGTTTTACTTGCTTTAAAAAACCTCCCACACCTCCCCCT
GAACCTGAAACATAAAATGAATGCAATTGTTGTTGTTAACTTGTTTATTGCAGCTTATAATGGTTACAAATAAAG
CAATAGCATCACAAATTTCACAAATAAAGCATTTTTTTCACTGCATTCTAGTTGTGGTTTGTCCAAACTCATCAA
TGTATCTTAACGCGTAAATTGTAAGCGTTAATATTTTGTTAAAATTCGCGTTAAATTTTTGTTAAATCAGCTCAT
TTTTTAACCAATAGGCCGAAATCGGCAAAATCCCTTATAAATCAAAAGAATAGACCGAGATAGGGTTGAGTGTTG
TTCCAGTTTGGAACAAGAGTCCACTATTAAAGAACGTGGACTCCAACGTCAAAGGGCGAAAAACCGTCTATCAGG
GCGATGGCCCACTACGTGAACCATCACCCTAATCAAGTTTTTTGGGGTCGAGGTGCCGTAAAGCACTAAATCGGA
ACCCTAAAGGGASCCCCGATTTAGAGCTTGACGGGGAAAGCCGGCGAACGTGCCA

6.4.2 Plasmid Sequence Maps

pEGFP-C3-hYAP1:

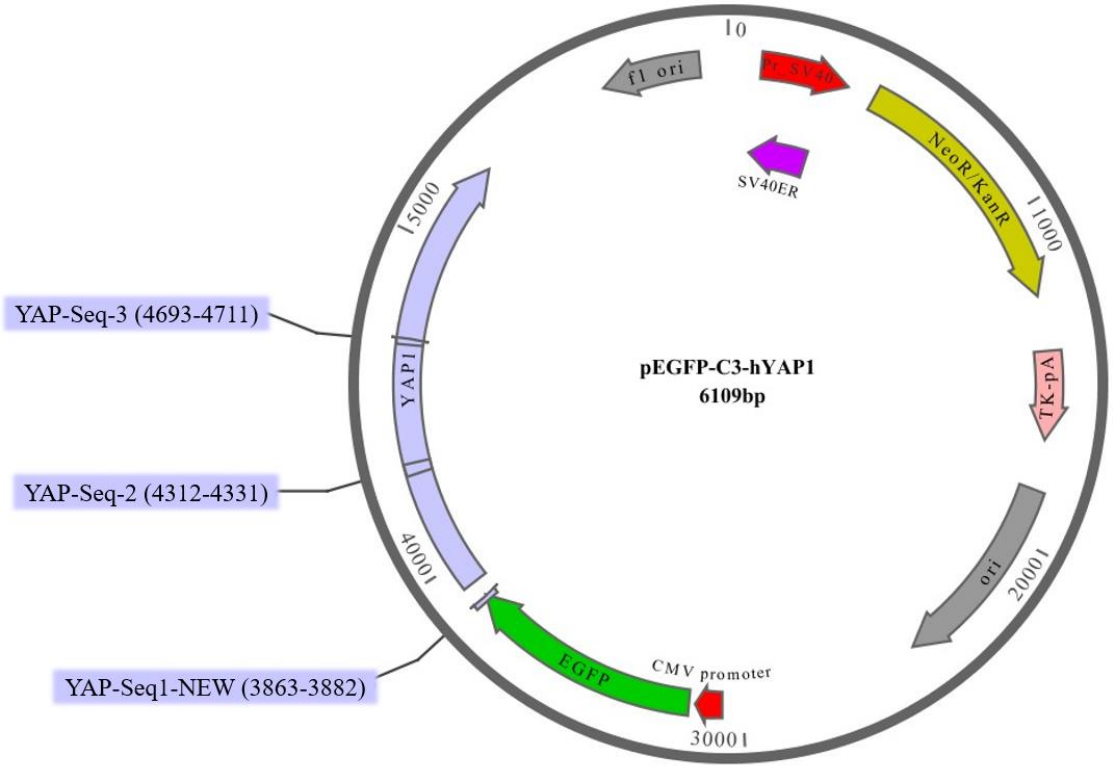

pEGFP-C3:

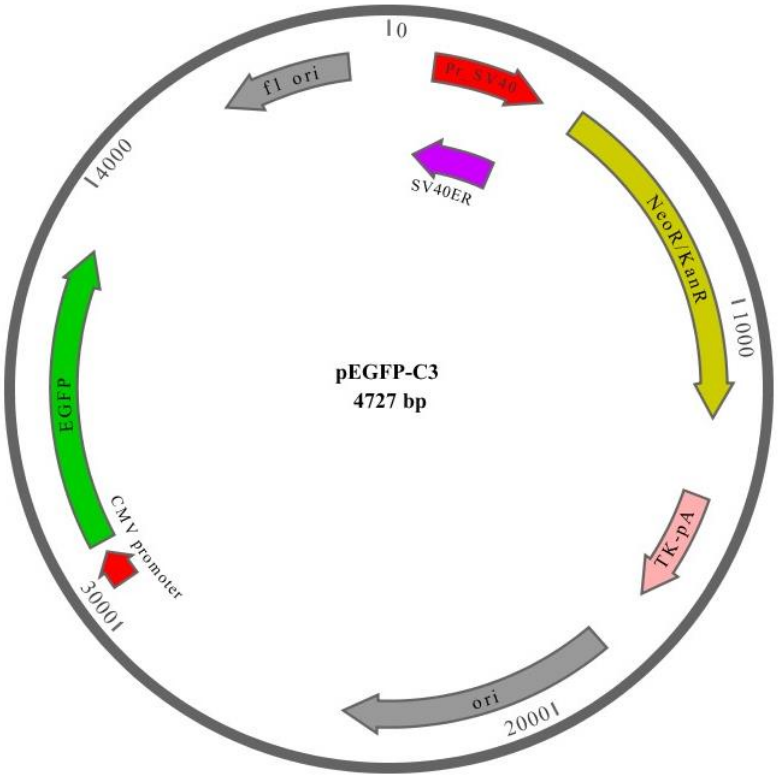

6.4.3 Immunofluorescence Results in Numbers

pEGFP-C3-hYAP1 WaGa	GFP	thereof Ki67
B1	172	170
B2	194	185
B3	200	188
Total	566	543
		95.57%

pEGFP-C3-hYAP1 PeTa	GFP	thereof Ki67
B1	121	97
B2	103	75
B3	88	74
Total	312	246
		79.02%

pEGFP-C3 WaGa	GFP	thereof Ki67
B1	144	127
B2	226	176
B3	173	75
Total	543	378
		69.81%

pEGFP-C3 PeTa	GFP	thereof Ki67
B1	257	150
B2	134	104
B3	51	20
Total	442	274
		58.39%

7 References

1. Hodgson NC. Merkel cell carcinoma: changing incidence trends. J Surg Oncol. 2005;89(1):1–4. doi:10.1002/jso.20167
2. Becker JC. Merkel cell carcinoma. Ann Oncol. 2010;21 Suppl 7vii81-5. doi:10.1093/annonc/mdq366
3. Stang A, Becker JC, Nghiem P, Ferlay J. The association between geographic location and incidence of Merkel cell carcinoma in comparison to melanoma: An international assessment. Eur J Cancer. 2018;9447–60. doi:10.1016/j.ejca.2018.02.003
4. Becker JC, Stang A, DeCaprio JA, Cerroni L, Lebbé C, Veness M, Nghiem P. Merkel cell carcinoma. Nat Rev Dis Primers. 2017;317077. doi:10.1038/nrdp.2017.77
5. Pellitteri PK, Takes RP, Lewis JS, Devaney KO, Harlor EJ, Strojan P, Rodrigo JP, Suárez C, Rinaldo A, Medina JE, Woolgar JA, Ferlito A. Merkel cell carcinoma of the head and neck. Head Neck. 2012;34(9):1346–54. doi:10.1002/hed.21787
6. Ma JE, Brewer JD. Merkel cell carcinoma in immunosuppressed patients. Cancers (Basel). 2014;6(3):1328–50. doi:10.3390/cancers6031328
7. Becker JC, Eigentler T, Frerich B, Gambichler T, Grabbe S, Höller U, Klumpp B, Loquai C, Krause-Bergmann A, Müller-Richter U, Pföhler C, Schneider-Burrus S, Stang A, Terheyden P, Ugurel S, Veith J, Mauch C. S2k guidelines for Merkel cell carcinoma (MCC, neuroendocrine carcinoma of the skin) - update 2018. J Dtsch Dermatol Ges. 2019;17(5):562–76. doi:10.1111/ddg.13841
8. Heath M, Jaimes N, Lemos B, Mostaghimi A, Wang LC, Peñas PF, Nghiem P. Clinical characteristics of Merkel cell carcinoma at diagnosis in 195 patients: the AEIOU features. J Am Acad Dermatol. 2008;58(3):375–81. doi:10.1016/j.jaad.2007.11.020
9. Feng H, Shuda M, Chang Y, Moore PS. Clonal integration of a polyomavirus in human Merkel cell carcinoma. Science. 2008;319(5866):1096–100. doi:10.1126/science.1152586
10. Houben R, Dreher C, Angermeyer S, Borst A, Utikal J, Haferkamp S, Peitsch WK, Schrama D, Hesbacher S. Mechanisms of p53 restriction in Merkel cell carcinoma cells are independent of the Merkel cell polyoma virus T antigens. J Invest Dermatol. 2013;133(10):2453–60. doi:10.1038/jid.2013.169
11. Fried I, Cerroni L. Merkel-Zell-Karzinom [Merkel cell carcinoma]. Pathologe. 2014;35(5):467–75. ger. doi:10.1007/s00292-014-1935-x
12. Pan D. The hippo signaling pathway in development and cancer. Dev Cell. 2010;19(4):491–505. doi:10.1016/j.devcel.2010.09.011
13. Gumbiner BM, Kim N-G. The Hippo-YAP signaling pathway and contact inhibition of growth. J Cell Sci. 2014;127(Pt 4):709–17. doi:10.1242/jcs.140103
14. Harvey KF, Zhang X, Thomas DM. The Hippo pathway and human cancer. Nat Rev Cancer. 2013;13(4):246–57. doi:10.1038/nrc3458

15. Mo J-S, Park HW, Guan K-L. The Hippo signaling pathway in stem cell biology and cancer. EMBO Rep. 2014;15(6):642–56. doi:10.15252/embr.201438638
16. Johnson R, Halder G. The two faces of Hippo: targeting the Hippo pathway for regenerative medicine and cancer treatment. Nat Rev Drug Discov. 2014;13(1):63–79. doi:10.1038/nrd4161
17. Halder G, Johnson RL. Hippo signaling: growth control and beyond. Development. 2011;138(1):9–22. doi:10.1242/dev.045500
18. Lai Z-C, Wei X, Shimizu T, Ramos E, Rohrbaugh M, Nikolaidis N, Ho L-L, Li Y. Control of cell proliferation and apoptosis by mob as tumor suppressor, mats. Cell. 2005;120(5):675–85. doi:10.1016/j.cell.2004.12.036
19. Tapon N, Harvey KF, Bell DW, Wahrer DCR, Schiripo TA, Haber DA, Hariharan IK. salvador Promotes both cell cycle exit and apoptosis in Drosophila and is mutated in human cancer cell lines. Cell. 2002;110(4):467–78. doi:10.1016/s0092-8674(02)00824-3
20. Piccolo S, Dupont S, Cordenonsi M. The biology of YAP/TAZ: hippo signaling and beyond. Physiol Rev. 2014;94(4):1287–312. doi:10.1152/physrev.00005.2014
21. Zanconato F, Cordenonsi M, Piccolo S. YAP/TAZ at the Roots of Cancer. Cancer Cell. 2016;29(6):783–803. doi:10.1016/j.ccell.2016.05.005
22. Moroishi T, Hansen CG, Guan K-L. The emerging roles of YAP and TAZ in cancer. Nat Rev Cancer. 2015;15(2):73–9. doi:10.1038/nrc3876
23. Halder G, Dupont S, Piccolo S. Transduction of mechanical and cytoskeletal cues by YAP and TAZ. Nat Rev Mol Cell Biol. 2012;13(9):591–600. doi:10.1038/nrm3416
24. Andl T, Zhou L, Yang K, Kadekaro AL, Zhang Y. YAP and WWTR1: New targets for skin cancer treatment. Cancer Lett. 2017;39630–41. doi:10.1016/j.canlet.2017.03.001
25. Debaugnies M, Sánchez-Danés A, Rorive S, Raphaël M, Liagre M, Parent M-A, Brisebarre A, Salmon I, Blanpain C. YAP and TAZ are essential for basal and squamous cell carcinoma initiation. EMBO Rep. 2018;19(7). doi:10.15252/embr.201845809
26. Nallet-Staub F, Marsaud V, Li L, Gilbert C, Dodier S, Bataille V, Sudol M, Herlyn M, Mauviel A. Pro-invasive activity of the Hippo pathway effectors YAP and TAZ in cutaneous melanoma. J Invest Dermatol. 2014;134(1):123–32. doi:10.1038/jid.2013.319
27. Basu S, Totty NF, Irwin MS, Sudol M, Downward J. Akt Phosphorylates the Yes-Associated Protein, YAP, to Induce Interaction with 14-3-3 and Attenuation of p73-Mediated Apoptosis. Molecular Cell. 2003;11(1):11–23. doi:10.1016/S1097-2765(02)00776-1
28. Guastafierro A, Feng H, Thant M, Kirkwood JM, Chang Y, Moore PS, Shuda M. Characterization of an early passage Merkel cell polyomavirus-positive Merkel cell carcinoma cell line, MS-1, and its growth in NOD scid gamma mice. J Virol Methods. 2013;187(1):6–14. doi:10.1016/j.jviromet.2012.10.001
29. van Gele M, Leonard JH, van Roy N, van Limbergen H, van Belle S, Cocquyt V, Salwen H, Paepe A de, Speleman F. Combined karyotyping, CGH and M-FISH analysis allows

detailed characterization of unidentified chromosomal rearrangements in Merkel cell carcinoma. Int J Cancer. 2002;101(2):137–45. doi:10.1002/ijc.10591

30. Rosen ST, Gould VE, Salwen HR, Herst CV, Le Beau MM, Lee I, Bauer K, Marder RJ, Andersen R, Kies MS. Establishment and characterization of a neuroendocrine skin carcinoma cell line. Lab Invest. 1987;56(3):302–12.
31. Wang Y, Xie C, Li Q, Xu K, Wang E. Clinical and prognostic significance of Yes-associated protein in colorectal cancer. Tumour Biol. 2013;34(4):2169–74. doi:10.1007/s13277-013-0751-x
32. Xia Y, Chang T, Wang Y, Liu Y, Li W, Li M, Fan H-Y. YAP promotes ovarian cancer cell tumorigenesis and is indicative of a poor prognosis for ovarian cancer patients. PLoS ONE. 2014;9(3):e91770. doi:10.1371/journal.pone.0091770
33. Perra A, Kowalik MA, Ghiso E, Ledda-Columbano GM, Di Tommaso L, Angioni MM, Raschioni C, Testore E, Roncalli M, Giordano S, Columbano A. YAP activation is an early event and a potential therapeutic target in liver cancer development. J Hepatol. 2014;61(5):1088–96. doi:10.1016/j.jhep.2014.06.033
34. Lau AN, Curtis SJ, Fillmore CM, Rowbotham SP, Mohseni M, Wagner DE, Beede AM, Montoro DT, Sinkevicius KW, Walton ZE, Barrios J, Weiss DJ, Camargo FD, Wong K-K, Kim CF. Tumor-propagating cells and Yap/Taz activity contribute to lung tumor progression and metastasis. EMBO J. 2014;33(5):468–81. doi:10.1002/embj.201386082
35. Jia J, Li C, Luo S, Liu-Smith F, Yang J, Wang X, Wang N, Lai B, Lei T, Wang Q, Xiao S, Shao Y, Zheng Y. Yes-Associated Protein Contributes to the Development of Human Cutaneous Squamous Cell Carcinoma via Activation of RAS. J Invest Dermatol. 2016;136(6):1267–77. doi:10.1016/j.jid.2016.02.005
36. Quan T, Xu Y, Qin Z, Robichaud P, Betcher S, Calderone K, He T, Johnson TM, Voorhees JJ, Fisher GJ. Elevated YAP and its downstream targets CCN1 and CCN2 in basal cell carcinoma: impact on keratinocyte proliferation and stromal cell activation. Am J Pathol. 2014;184(4):937–43. doi:10.1016/j.ajpath.2013.12.017
37. Feng Q, Guo P, Kang S, Zhao F. High expression of TAZ/YAP promotes the progression of malignant melanoma and affects the postoperative survival of patients. Pharmazie. 2018;73(11):662–5. doi:10.1691/ph.2018.8499
38. Sanchez IM, Aplin AE. Hippo: hungry, hungry for melanoma invasion. J Invest Dermatol. 2014;134(1):14–6. doi:10.1038/jid.2013.372
39. Xiong H, Yu Q, Gong Y, Chen W, Tong Y, Wang Y, Xu H, Shi Y. Yes-Associated Protein (YAP) Promotes Tumorigenesis in Melanoma Cells Through Stimulation of Low-Density Lipoprotein Receptor-Related Protein 1 (LRP1). Sci Rep. 2017;7(1):15528. doi:10.1038/s41598-017-14764-4
40. Dong X, Meng L, Liu P, Ji R, Su X, Xin Y, Jiang X. YAP/TAZ: a promising target for squamous cell carcinoma treatment. Cancer Manag Res. 2019;116245–52. doi:10.2147/CMAR.S197921
41. Popp S, Waltering S, Herbst C, Moll I, Boukamp P. UV-B-type mutations and chromosomal imbalances indicate common pathways for the development of Merkel

and skin squamous cell carcinomas. Int J Cancer. 2002;99(3):352–60. doi:10.1002/ijc.10321

42. Gomez LG, DiMaio S, Silva EG, Mackay B. Association between neuroendocrine (Merkel cell) carcinoma and squamous carcinoma of the skin. Am J Surg Pathol. 1983;7(2):171–7. doi:10.1097/00000478-198303000-00007
43. Nassios A, Wallner S, Haferkamp S, Klingelhöffer C, Brochhausen C, Schreml S. Expression of proton-sensing G-protein-coupled receptors in selected skin tumors. Exp Dermatol. 2019;28(1):66–71. doi:10.1111/exd.13809
44. Gambichler T, Ardabili S, Dreißigacker M, Scheel CH, Brand-Saberi B, Skrygan M, Stockfleth E, Becker JC. Expression of Lefty predicts Merkel cell carcinoma-specific death. J Eur Acad Dermatol Venereol. 2020. doi:10.1111/jdv.16271
45. Liu S, Daa T, Kashima K, Kondoh Y, Yokoyama S. The Wnt-signaling pathway is not implicated in tumorigenesis of Merkel cell carcinoma. J Cutan Pathol. 2007;34(1):22–6. doi:10.1111/j.1600-0560.2006.00577.x
46. García P, Rosa L, Vargas S, Weber H, Espinoza JA, Suárez F, Romero-Calvo I, Elgueta N, Rivera V, Nervi B, Obreque J, Leal P, Viñuela E, Aguayo G, Muñiz S, Sagredo A, Roa JC, Bizama C. Hippo-YAP1 Is a Prognosis Marker and Potentially Targetable Pathway in Advanced Gallbladder Cancer. Cancers (Basel). 2020;12(4). doi:10.3390/cancers12040778
47. Guo L, Teng L. YAP/TAZ for cancer therapy: opportunities and challenges (review). Int J Oncol. 2015;46(4):1444–52. doi:10.3892/ijo.2015.2877
48. Houben R, Shuda M, Weinkam R, Schrama D, Feng H, Chang Y, Moore PS, Becker JC. Merkel cell polyomavirus-infected Merkel cell carcinoma cells require expression of viral T antigens. J Virol. 2010;84(14):7064–72. doi:10.1128/JVI.02400-09
49. Daily K, Coxon A, Williams JS, Lee C-CR, Coit DG, Busam KJ, Brownell I. Assessment of cancer cell line representativeness using microarrays for Merkel cell carcinoma. J Invest Dermatol. 2015;135(4):1138–46. doi:10.1038/jid.2014.518
50. Zhao B, Li L, Wang L, Wang C-Y, Yu J, Guan K-L. Cell detachment activates the Hippo pathway via cytoskeleton reorganization to induce anoikis. Genes Dev. 2012;26(1):54–68. doi:10.1101/gad.173435.111
51. Liberio MS, Sadowski MC, Soekmadji C, Davis RA, Nelson CC. Differential effects of tissue culture coating substrates on prostate cancer cell adherence, morphology and behavior. PLoS ONE. 2014;9(11):e112122. doi:10.1371/journal.pone.0112122
52. Harnett EM, Alderman J, Wood T. The surface energy of various biomaterials coated with adhesion molecules used in cell culture. Colloids Surf B Biointerfaces. 2007;55(1):90–7. doi:10.1016/j.colsurfb.2006.11.021
53. Leonard JH, Dash P, Holland P, Kearsley JH, Bell JR. Characterisation of four Merkel cell carcinoma adherent cell lines. Int J Cancer. 1995;60(1):100–7. doi:10.1002/ijc.2910600115

54. Leonard JH, Bell JR. Insights into the Merkel cell phenotype from Merkel cell carcinoma cell lines. Australas J Dermatol. 1997;38 Suppl 1S91-8. doi:10.1111/j.1440-0960.1997.tb01019.x

55. Shi B, Xue M, Wang Y, Wang Y, Li D, Zhao X, Li X. An improved method for increasing the efficiency of gene transfection and transduction. Int J Physiol Pathophysiol Pharmacol. 2018;10(2):95–104.

56. Wang T, Larcher LM, Ma L, Veedu RN. Systematic Screening of Commonly Used Commercial Transfection Reagents towards Efficient Transfection of Single-Stranded Oligonucleotides. Molecules. 2018;23(10). doi:10.3390/molecules23102564

57. Rahimi P, Mobarakeh VI, Kamalzare S, SajadianFard F, Vahabpour R, Zabihollahi R. Comparison of transfection efficiency of polymer-based and lipid-based transfection reagents. Bratisl Lek Listy. 2018;119(11):701–5. doi:10.4149/BLL_2018_125

58. Gonzalez Villarreal C, Said Fernandez S, Soto Dominguez A, Padilla Rivas G, Garza Treviño E, Rodriguez Rocha H, Martinez Rodriguez H. Bone marrow mesenchymal stem cells: improving transgene expression level, transfection efficiency and cell viability. J BUON. 2018;23(6):1893–903.

59. van Gele M, Kaghad M, Leonard JH, van Roy N, Naeyaert JM, Geerts ML, van Belle S, Cocquyt V, Bridge J, Sciot R, Wolf-Peeters C de, Paepe A de, Caput D, Speleman F. Mutation analysis of P73 and TP53 in Merkel cell carcinoma. Br J Cancer. 2000;82(4):823–6. doi:10.1054/bjoc.1999.1006

60. Goh G, Walradt T, Markarov V, Blom A, Riaz N, Doumani R, Stafstrom K, Moshiri A, Yelistratova L, Levinsohn J, Chan TA, Nghiem P, Lifton RP, Choi J. Mutational landscape of MCPyV-positive and MCPyV-negative Merkel cell carcinomas with implications for immunotherapy. Oncotarget. 2016;7(3):3403–15. doi:10.18632/oncotarget.6494

61. Weeraratna AT, Houben R, O'Connell MP, Becker JC. Lack of Wnt5A expression in Merkel cell carcinoma. Arch Dermatol. 2010;146(1):88–9. doi:10.1001/archdermatol.2009.348

62. Strong S, Shalders K, Carr R, Snead DRJ. KIT receptor (CD117) expression in Merkel cell carcinoma. Br J Dermatol. 2004;150(2):384–5. doi:10.1111/j.1365-2133.2003.05779.x

63. Feinmesser M, Halpern M, Kaganovsky E, Brenner B, Fenig E, Hodak E, Sulkes J, Okon E. c-kit expression in primary and metastatic merkel cell carcinoma. Am J Dermatopathol. 2004;26(6):458–62. doi:10.1097/00000372-200412000-00003

64. Llombart B, Monteagudo C, López-Guerrero JA, Carda C, Jorda E, Sanmartín O, Almenar S, Molina I, Martín JM, Llombart-Bosch A. Clinicopathological and immunohistochemical analysis of 20 cases of Merkel cell carcinoma in search of prognostic markers. Histopathology. 2005;46(6):622–34. doi:10.1111/j.1365-2559.2005.02158.x

65. Brunner M, Thurnher D, Pammer J, Geleff S, Heiduschka G, Reinisch CM, Petzelbauer P, Erovic BM. Expression of VEGF-A/C, VEGF-R2, PDGF-alpha/beta, c-kit, EGFR, Her-2/Neu, Mcl-1 and Bmi-1 in Merkel cell carcinoma. Mod Pathol. 2008;21(7):876–84. doi:10.1038/modpathol.2008.63

66. Swick BL, Ravdel L, Fitzpatrick JE, Robinson WA. Merkel cell carcinoma: evaluation of KIT (CD117) expression and failure to demonstrate activating mutations in the C-KIT proto-

oncogene - implications for treatment with imatinib mesylate. J Cutan Pathol. 2007;34(4):324–9. doi:10.1111/j.1600-0560.2006.00613.x

67. Swick BL, Srikantha R, Messingham KN. Specific analysis of KIT and PDGFR-alpha expression and mutational status in Merkel cell carcinoma. J Cutan Pathol. 2013;40(7):623–30. doi:10.1111/cup.12160
68. Worda M, Sreevidya CS, Ananthaswamy HN, Cerroni L, Kerl H, Wolf P. T1796A BRAF mutation is absent in Merkel cell carcinoma. Br J Dermatol. 2005;153(1):229–32. doi:10.1111/j.1365-2133.2005.06713.x
69. Houben R, Michel B, Vetter-Kauczok CS, Pföhler C, Laetsch B, Wolter MD, Leonard JH, Trefzer U, Ugurel S, Schrama D, Becker JC. Absence of classical MAP kinase pathway signalling in Merkel cell carcinoma. J Invest Dermatol. 2006;126(5):1135–42. doi:10.1038/sj.jid.5700170
70. Kennedy MM, Blessing K, King G, Kerr KM. Expression of bcl-2 and p53 in Merkel cell carcinoma. An immunohistochemical study. Am J Dermatopathol. 1996;18(3):273–7. doi:10.1097/00000372-199606000-00006
71. Plettenberg A, Pammer J, Tschachler E. Merkel cells and Merkel cell carcinoma express the BCL-2 proto-oncogene. Exp Dermatol. 1996;5(3):183–8. doi:10.1111/j.1600-0625.1996.tb00114.x
72. Feinmesser M, Halpern M, Fenig E, Tsabari C, Hodak E, Sulkes J, Brenner B, Okon E. Expression of the apoptosis-related oncogenes bcl-2, bax, and p53 in Merkel cell carcinoma: Can they predict treatment response and clinical outcome? Hum Pathol. 1999;30(11):1367–72. doi:10.1016/s0046-8177(99)90070-9
73. Liu W, Krump NA, Herlyn M, You J. Combining DNA Damage Induction with BCL-2 Inhibition to Enhance Merkel Cell Carcinoma Cytotoxicity. Biology (Basel). 2020;9(2). doi:10.3390/biology9020035
74. Hafner C, Houben R, Baeurle A, Ritter C, Schrama D, Landthaler M, Becker JC. Activation of the PI3K/AKT pathway in Merkel cell carcinoma. PLoS ONE. 2012;7(2):e31255. doi:10.1371/journal.pone.0031255
75. Starrett GJ, Marcelus C, Cantalupo PG, Katz JP, Cheng J, Akagi K, Thakuria M, Rabinowits G, Wang LC, Symer DE, Pipas JM, Harris RS, DeCaprio JA. Merkel Cell Polyomavirus Exhibits Dominant Control of the Tumor Genome and Transcriptome in Virus-Associated Merkel Cell Carcinoma. mBio. 2017;8(1). doi:10.1128/mBio.02079-16

8 Danksagung

An dieser Stelle möchte ich allen Menschen danken, die mich bei der Anfertigung meiner Dissertation unterstützt haben.

Besonders möchte ich mich bei Herrn Priv.-Doz. Dr. Sebastian Haferkamp für die Überlassung dieses interessanten Themas und die hervorragende Betreuung bedanken. Die großartige Unterstützung und die erfolgreiche Zusammenarbeit haben mir die Erstellung meiner Dissertation sehr erleichtert.

Ein weiterer großer Dank geht an Frau Barbara Schwertner für die ausgezeichnete Betreuung, die unermüdliche Unterstützung bei der Planung der Experimente und der Versuchsdurchführung und dafür, stets als Ansprechpartnerin für mich da zu sein. Abermals vielen Dank für das herzliche Willkommenheißen und Einarbeiten im Labor, die guten Ratschläge, produktiven Gespräche und lieben Worte auf dem Weg zu meiner Dissertation.

Des Weiteren möchte ich mich bei Frau Susanne Wallner für die Unterstützung bei der Versuchsdurchführung bedanken und dafür, dass sie stets als liebenswerte Hilfe für mich da war.

Ich möchte mich von ganzem Herzen bei meiner Familie bedanken, da sie mir immer mit Geduld, Ermutigungen und Zuspruch zur Seite stand. Mein herzlichster Dank geht an meine Geschwister Martin Hoffmann und Andrea Laubichler, sowie an Frank Kienast dafür, dass sie mir in jeder Lebenslage weiterhelfen. Abschließend geht mein größter Dank an meine Eltern, die immer für mich da sind, und ohne deren Unterstützung mein Studium sowie die Erstellung dieser Arbeit nicht möglich gewesen wären.

9 Eidesstattliche Erklärung

Hiermit erkläre ich, Monika Dorothee Hoffmann, dass ich die vorliegende Arbeit ohne unzulässige Hilfe Dritter und ohne Benutzung anderer als der angegebenen Hilfsmittel angefertigt habe. Die aus anderen Quellen direkt oder indirekt übernommenen Daten und Konzepte sind unter Angabe der Quelle gekennzeichnet. Insbesondere habe ich nicht die entgeltliche Hilfe von Vermittlungs-bzw. Beratungsdiensten (Promotionsberater oder andere Personen) in Anspruch genommen. Niemand hat von mir unmittelbar oder mittelbar geldwerte Leistungen für Arbeit erhalten, die im Zusammenhang mit dem Inhalt der vorgelegten Dissertation stehen. Die Arbeit wurde bisher weder im In-noch im Ausland in gleicher oder ähnlicher Form einer anderen Prüfungsbehörde vorgelegt.

Monika Dorothee Hoffmann Regensburg den 08.12.2020